Fall 2022

Biomimetic Synthesis of Palladium Nanoparticles for Catalytic Application

Emily A. Groover

BIOMIMETIC SYNTHESIS OF PALLADIUM NANOPARTICLES FOR CATALYTIC APPLICATION

by

EMILY GROOVER

(Under the Direction of Beverly Penland)

ABSTRACT

The synthesis of palladium nanoparticles (Pd NPs) using materials-directed peptides is a novel, nontoxic approach which exerts a high level of control over the particle size and shape. This biomimetic technique is environmentally benign, featuring nonhazardous ligands and ambient conditions. Nanoparticles are extremely reactive catalysts, boasting a large surface-to-volume ratio when compared to their bulk counterparts. The rational design of these nanoparticles using peptides has been very successful in aqueous environments, but no research has been done to apply it in organic systems. As such, the biomimetic synthesis of Pd NPs in an organic system is here investigated, with ethanol and dimethyl sulfoxide (DMSO) as solvents of interest. These systems adapt palladium-binding peptides to incorporate a hydrophobic region on the -N terminus, -C terminus, and both N and C termini to aid in solvent interaction during nanoparticle synthesis. These peptides proved to successfully synthesize colloidal nanoparticles in both ethanol and DMSO. Their subsequent application as catalysts in the Suzuki-Miyaura carbon cross-coupling reaction facilitated a comparison of the peptide-capped nanoparticles' catalytic activity. Catalytic studies indicate that the S2Pd4S2 peptide, with two hydrophobic regions, produced nanoparticles with the highest catalytic activity as compared to the other major peptides, suggesting that materials-directed peptides may be adapted and tuned to operate effectively in organic solvents.

INDEX WORDS: Peptides, Biomimetic Synthesis, Palladium, Nanoparticles, Catalysts, Suzuki-Miyaura, Cross-coupling

BIOMIMETIC SYNTHESIS OF PALLADIUM NANOPARTICLES FOR CATALYTIC APPLICATION

by

EMILY GROOVER

B.S., Georgia Southern University, 2021

A Thesis Submitted to the Graduate Faculty of Georgia Southern University

in Partial Fulfillment of the Requirements of the Degree

MASTER OF SCIENCE

BIOMIMETIC SYNTHESIS OF PALLADIUM NANOPARTICLES FOR CATALYTIC APPLICATION

by

EMILY GROOVER

Major Professor: Beverly Penland

Committee: Brandon Quillian

Mitch Weiland

Electronic Version Approved: December 2022

DEDICATION

This work is dedicated to my first teacher, Tracy Wells.

ACKNLOWLEDGMENTS

I would like to acknowledge the leadership and direction of Dr. Beverly Penland throughout the execution of this work. I would also like to extend sincere appreciation to Dr. Brandon Quillian for his mentorship and guidance throughout all stages of this project. I acknowledge the significant contributions of the Chemistry and Biochemistry department in logistical lab management and instrumentation use. I also acknowledge the contributions of both Dr. Mitch Weiland and Dr. Brandon Quillian for their roles on my thesis committee. Finally, I would like to acknowledge the ACS Petroleum Research Fund for their financial support of this research effort.

TABLE OF CONTENTS

Page

DEDICATION……..2

ACKNOWLEDGMENTS.....3

LIST OF FIGURES 6

LIST OF TABLES 8

CHAPTER

1. INTRODUCTION ……..……..9

1.1 Purpose of the study ..…….……....9

1.2 Palladium Noble Metal ..…..……..10

1.2.1 Global Supply ……..10

1.2.2 Applications in Catalysis……..11

1.3 Palladium Nanoparticles……11

1.3.1 Advantages as Catalysts…….……..11

1.3.2 Synthesis ……..11

1.4 Ligand Innovation……..12

1.4.1 Biomolecular Ligands..……14

1.5 Peptide Ligands for Nanoparticle Synthesis……..15

1.5.1 Peptide Specificity ……...18

1.5.2 Peptide Tunability .……...20

1.6 Peptide-capped Pd Nanoparticle Synthesis in Organic Solvents……...22

1.6.1 Bifunctional Peptides for Organic Applications……...22

1.7 Pd Nanoparticles in Catalysis……24

1.7.1. Factors in Catalytic Activity...……..25

1.7.2 Pd NP Catalytic Mechanism...……..26

2 ETHANOL STUDIES ……..……...……28

2.1 Method of Synthesis……...28

2.2 Characterization of Nanoparticles in Ethanol ……..……...…...……...……..29

2.3 Catalytic Application of Nanoparticles Synthesized in Ethanol ……32

2.3.1 24-Hour Suzuki-Miyaura Studies at 0.05 mol% Pd …….…….32

2.3.2 Turnover Frequency (TOF) Studies of Suzuki-Miyaura Reaction…..……..37

3 DMSO STUDIES ……..……...41

3.1 Synthesis and Characterization of Nanoparticles in DMSO ……..41

3.2 Catalytic Application of Nanoparticles Synthesized in DMSO …….44

3.2.1 24-Hour Suzuki-Miyaura Studies at 0.05 mol% Pd …..……44

3.2.2 Turnover Frequency (TOF) Studies of Suzuki-Miyaura Reaction……....47

4 CONCLUSION ……..……..50

REFERENCES……53

LIST OF FIGURES

Figure 1. Global palladium supply and demand analysis…….10

Figure 2. Structure of triphenyl phosphine……..13

Figure 3. (A) Repeating unit (N-vinylpyrrolidone) of the synthetic polymer PVP. (B) General chemical structure of poly(amido-amine) dendrimer……..…….…..14

Figure 4. Inorganic morphologies of Au and Pd nanomaterials generated by DNA……15

Figure 5. Silica-based nanostructures of diatoms found in nature…….…...16

Figure 6. Magnetotactic bacteria containing magnetite crystals synthesized in a linear arrangement…...16

Figure 7. Schematic for peptide-mediated palladium nanoparticle synthesis in water……...17

Figure 8. Schematic of phage display…….……..19

Figure 9. Depiction of the 'kinked' binding moiety of Pd4……..……...19

Figure 10. Schematic of the facet-directed peptide-mediated synthesis of platinum nanostructures……...21

Figure 11. Chemdraw illustration of the Pd4 peptide (TSNAVHPTLRHL)…….....22

Figure 12. Chemdraw illustration of the S2 peptide……24

Figure 13. Basic line reaction for Suzuki-Miyaura carbon cross-coupling reaction..…….25

Figure 14. General schematic of the Suzuki-Miyaura mechanism for aryl-aryl coupling……27

Figure 15. UV-Vis spectra (complexed and reduced) for Pd nanoparticles synthesized in ethanol…….29

Figure 16. TEM images for Pd nanoparticles synthesized in ethanol……..30

Figure 17. Specific parameters for the 24-Hr Suzuki-Miyaura reaction……..33

Figure 18. Single-pulse, high yield proton NMR of 24-Hr Suzuki reaction utilizing Pd NPs synthesized in ethanol……..34

Figure 19. Verification of Suzuki product via gas chromatogram…….……..34

Figure 20. Verification of Suzuki product via mass spectrum…….35

Figure 21. Average percent yields determined from the 24-hour Suzuki reaction using Pd NPs synthesized in ethanol from the three major peptides……..……35

Figure 22. Average percent yields determined from the 24-hour Suzuki reaction using Pd NPs synthesized in ethanol from the two control peptides……..36

Figure 23. Graph of the linear progression of the Suzuki-Miyaura reaction over 2.5 hours…….38

Figure 24. UV-Vis spectra (complexed & reduced) for Pd nanoparticles synthesized in DMSO...41

Figure 25. TEM images for Pd nanoparticles synthesized in DMSO…….……42

Figure 26. Resonance structures of DMSO…….43

Figure 27. Single-pulse, high yield proton NMR of 24-Hr Suzuki reaction utilizing Pd NPs synthesized in DMSO……..44

Figure 28. Average percent yields determined from the 24-hour Suzuki reaction using Pd NPs synthesized in DMSO from the three major peptides and their respective ratios.…….……..45

Figure 29. Average percent yields determined from the 24-hour Suzuki reaction using Pd NPs synthesized in DMSO from the two control peptides and their respective ratios…….45

Figure 30. Graph of the linear progression of the Suzuki-Miyaura reaction over 4 hours……..47

Figure 31. TEM images of nanoparticles produced by the S2 peptide in DMSO ……..49

LIST OF TABLES

Table 1. Peptide library with alanine substitutions at positions 6 and 11 with corresponding Pd NP sizes for various Pd/peptide ratios…….20

Table 2. Amino acid sequences for two control and three bifunctional peptides used in NP synthesis……28

Table 3. Average size determinations (nm) for Pd NPs synthesized in ethanol……31

Table 4. Peptides and ratios synthesized in ethanol with the highest reactivity determined by the 24-hour Suzuki studies……..…..38

Table 5. Turnover Frequency values for Pd NPs synthesized in ethanol…….……39

Table 6. Average product yield at 2.5-hour mark for Pd NPs synthesized in ethanol…….39

Table 7. Average size determinations for the most reactive Pd NPs synthesized in DMSO…….42

Table 8. Turnover Frequency values for the Pd NPs synthesized in DMSO with optimal peptide and ratio combinations as determined by the 24-hour studies……..……48

Table 9. Average product yield at 2-hour mark for Pd NPs synthesized in DMSO using optimal peptide and ratio combinations……...……..48

CHAPTER 1

INTRODUCTION

In the world of organic chemistry, transition metal catalyzed carbon cross-coupling (C-C) reactions are essential for the preparation of value-added molecules.[1, 2] These reactions are exponentially more effective when palladium nanoparticles (Pd NPs) are used instead of their bulk counterparts due to their increased surface area-to-volume ratio.[3-6] Because of a global deficit in palladium supply, nanoscale methods which boast low catalyst material loading are necessary for the improved management of Pd as a natural resource.[7] As such, sustainable Pd nanoparticle design has been a specific area of interest for researchers in the last decade. Peptide-mediated synthesis has proven to be quite successful, exerting a high level of control over Pd NP size and shape.[6, 8-10] Additionally, the peptide-based system's conditions are ambient, with no added heat or pressure. Previous successes in aqueous media suggest that the synthesis of peptide-capped Pd NPs may be translated to organic systems, making them more relevant for industrial use.[5] Further, a 'green' approach prioritizes solvents of synthesis with minimal health and environmental impacts. To translate the catalytic efficiency and minimal toxicity of Pd NP synthesis from aqueous to organic systems, the peptide used for synthesis must be compatible with organic solvents. Peptide sequence alteration here allows for the synthesis of bifunctional peptides, which maintain the coordination specificity for palladium and interact well with organic solvents during nanoparticle synthesis.

1.1 Purpose of the study

This research project is focused on the rational design and biomimetic synthesis of peptide-capped palladium nanoparticles in organic solvents for catalytic application in the Suzuki-Miyaura cross-coupling reaction. The investigated solvents were ethanol and DMSO. The synthesis was achieved through peptide-mediated nanoparticle assembly, in which bifunctional peptides with specific affinity for palladium served to cap growing Pd particles in solution, halting their growth and producing nanoparticles with specific size

and shape. The catalytic application of the Pd NPs in the Suzuki reaction allowed for a comparison of the effects of each peptide system on the activity of the nanoparticles produced.

1.2 Palladium Noble Metal

1.2.1 Global Supply

Palladium is a transition metal first discovered in 1803 by William Hyde Wollaston of Brazil.[11] He experimented on residues left from dissolving platinum in aqua regia and after a series of reactions and heating processes, extracted palladium metal. Today most palladium exists within deposits of platinum, nickel, gold, and other precious metals, requiring special mining, extraction, and separation techniques to separate Pd from other elements.[12] Although palladium is not considered as precious as gold or silver, its price has risen over 300% since 2016 due to a supply and demand imbalance.[7] In 2021, over 21 metric tons of palladium was applied in the chemical catalyst industry, accounting for 7% of global consumption.[13] Due to this high demand, there is now a supply deficit of palladium (see Figure 1).[7] This has initiated a movement to optimize palladium usage through sustainable research efforts which are especially relevant in the biomedical and pharmaceutical industries.

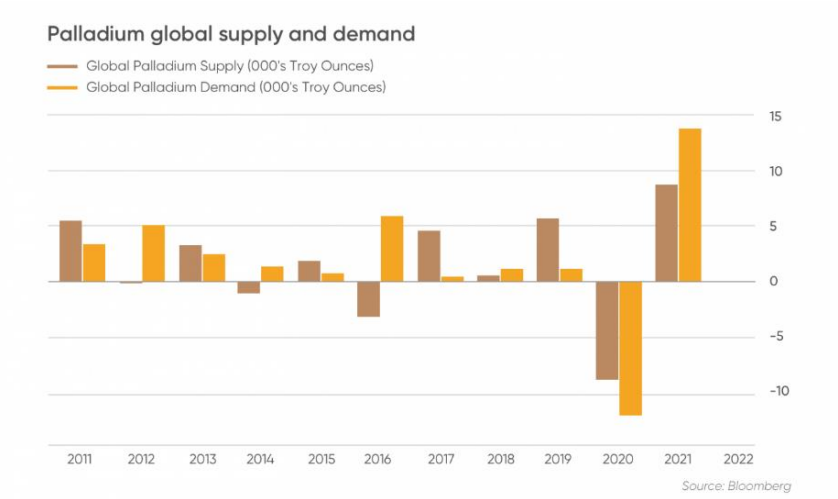

Figure 1. Global palladium supply and demand analysis. Report is from January 2011- June 2021, measured in troy ounces, an internationally standardized weight measurement. From reference 7.

1.2.2 Applications in Catalysis

Historically, palladium has been called the king of transition-metal catalysts, with applications in hydrogenation and carbon cross-coupling reactions.[14] Palladium has strong tendencies to form bonds with carbon and is considered very active in its +2 and 0 oxidation states.[15] This is due to its unoccupied d-orbitals which stand ready to receive electrons, attaining stable d^{10} or d^{8} electron configurations. Among the myriad of reactions in organic synthesis, palladium catalyzed cross-coupling (C-C) reactions are known to be extremely successful, with a variety of applications and substrates.

1.3 Palladium Nanoparticles

1.3.1 Advantages as catalysts

Most catalyst systems employ bulk palladium catalysts, however a more sustainable catalyst design would be both financially and environmentally advantageous.[2] Research has shown that Pd nanoparticle catalysts are exponentially more effective than their bulk counterparts. This is due to their maximized surface area-to-volume ratio which reduces the necessary catalyst loading to promote activity.[3-6] Additionally, the intricate surface structures of Pd NPs exhibit atomic-level ridges and grooves which can serve as active sites for catalytic activity.[16] The crystal structure of metal nanoparticles may result in high or low-index surfaces which also contribute to their catalytic efficiency.[16] The interest in Pd-based nanomaterials as highly active and stable catalysts has ultimately spawned from a global need to support anthropogenic energy demands in sectors of pharmaceutical development and fine chemical synthesis.[3] Pd nanoparticles have been synthesized through both industrial processes and natural mechanisms.[14, 17, 18]

1.3.2 Synthesis

Palladium nanoparticles are currently synthesized on an industrial scale for a variety of applications including catalysis, drug delivery and medical diagnostics.[1-3] Synthesis routes typically use a top-down or

bottom-up approach. The top-down approach breaks down or sculpts bulk material into nanosized particles without molecular rearrangement. This often occurs through physical methods such as mechanical milling or laser ablation.[4, 19] The bottom-up approach features the assembly and coordination of atomic-scale metal precursors in the gas, liquid or solid phase. Physical preparation methods may include hydrothermal or electron-beam deposition, powder or aerosol compaction, and gas spray pyrolysis.[19] Nearly all methods used for the industrial synthesis of Pd NPs involve energy-intensive processes and environmentally toxic solvents, and they often produce nanoparticles with inconsistent size and shape.[2, 4, 20] Interestingly, the synthesis method of chemical reduction has been shown to produce unique Pd nanostructures in addition to spherical particles, including nanocubes, nanowires, nanorods and nanotubes.[19] Chemical reduction methods include electrochemical deposition, microemulsions, and photochemical synthesis, all of which may tune their synthesis parameters in order to achieve different product morphologies.[20] This type of nanoparticle tunability is considered nonspecific and is based upon the synthesis conditions, the presence of stabilizers and the type of reducing agent used to initiate nucleation.[20] The synthesis conditions may involve different types of solutions or a dry deposition of metal materials. In addition, a stabilizer such as a metal sheet or plate may be used to support the growing nanostructures, or a ligand which coordinates with growing nanoparticles while suspended in a solution.[2, 20] Finally, a strong reducing agent may initiate nucleation of the Pd atoms much faster than a weaker reducing agent, thus affecting the final structure of the nanomaterial. Chemical reduction is a technique similar to the work being done in this research, however in an industrial setting, it, like nearly every other industrial synthesis technique, does not meet sustainability objectives. Thus, there is a pressing need to optimize Pd NP synthesis to increase cost-effectiveness, minimize toxicity, and reduce energy input.

1.4 Ligand Innovation

One of the most significant areas of applied research in nanoparticle synthesis is that of ligand innovation.[2] Ligands and other stabilizing agents are critical for obtaining NPs of suitable size and for

preventing aggregation of Pd^0 atoms into palladium black. Ligand coordination with metal atoms often occurs through interaction between a lone pair of electrons and the transition metal's unoccupied d-orbitals. This interaction stabilizes the final surface structure and impacts the reactivity of the nanoparticles produced. Until 1998, most reaction systems utilized triphenylphosphine ligands (see Figure 2) to stabilize palladium catalysts.[21] Metal-phosphine compounds are known to be extremely hazardous, often classified with the signal word 'danger'.[22] Exposure effects range from cellular poisoning and oxidative stress to overall metabolic disruption.[23] In addition, metal phosphides are known to produce toxic phosphine gas upon degradation which often results in a negative environmental impact, incurring high disposal costs.[23] For these reasons, extensive research has been done in the field of nanocatalysts regarding ligand design.[2] Considerable focus has been given to the optimization of traditional Pd NP synthesis by investigating tunable ligand systems which are environmentally friendly and which would minimize any hazards associated with synthesis and disposal.[6, 21] Developments in nanotechnology have also sparked investigations into the unique physiochemical interactions between transition metal nanoparticles and their supporting ligands, as these significantly impact the final NP surface structure, the amount of exposed Pd, and thus the overall catalytic activity.[4]

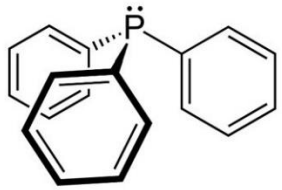

Figure 2: Structure of triphenyl phosphine. From reference 21.

In recent years, non-toxic ligand alternatives for Pd NP synthesis have shown significant promise and the potential to operate well under ambient conditions. These variations have been shown to maintain quantitative yields in catalytic applications, proving that the prioritization of 'green' synthesis methods does

not compromise efficiency.[24, 25] These ligands include polymers, dendrimers, and biomolecules.[3] Reetz *et. al* were one of the first research groups to synthesize Pd NPs using polyvinylpyrrolidone (PVP) a water-soluble, amorphous, synthetic polymer made from N-vinylpyrrolidone (see Figure 3A).[3, 25, 26] Another group led by researcher El-Sayed synthesized Pd NPs using poly(amido-amine) dendrimers dubbed G2, G3 and G4 as a means of steric stabilization (see Figure 3B).[3, 24]

A **B**

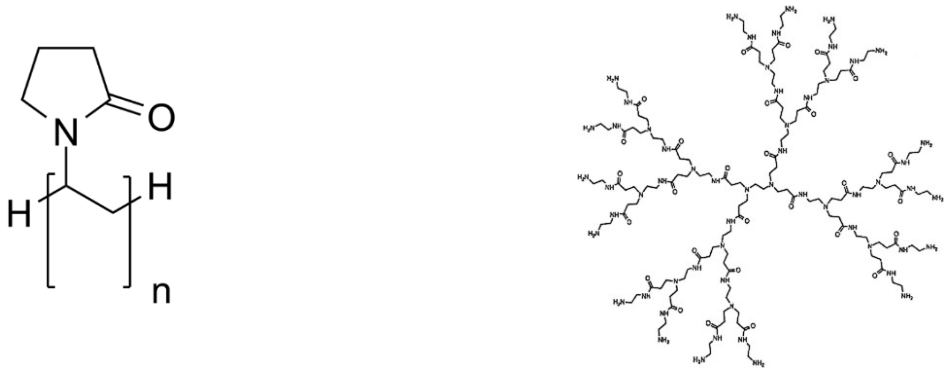

Figure 3. (A) Repeating unit (N-vinylpyrrolidone) of the synthetic polymer PVP. **(B)** General chemical structure of poly(amido-amine) dendrimer. From references 23 and 25.

1.4.1 Biomolecular Ligands

In addition to synthetic polymers, biological molecules such as DNA and peptides have also been successfully employed as ligands to produce inorganic nanomaterials.[27] Specific DNA sequences have been shown to generate Au, Ag and Pd/Au nanoparticles in which singular base substitutions resulted in unique nanostructures.[27] As seen in Figure 4A, when adenine is positioned at the 20th residue on the DNA backbone, a dumbbell shaped nanostructure is produced. When thymine or cytosine is substituted, a trigonal bipyramidal structure results, and a guanine substitution results in additional space between the two pyramidal ends. In Figure 4B, thymine, adenine, cysteine, and guanine substitutions at the 10th residue have different directing effects on the growing particles, resulting in fine alterations to the faces and ridges of the different nanoparticles produced. Unfortunately, the application of DNA for research in nanoparticle synthesis is limited. The financial cost of synthesizing DNA can be difficult to sustain, the rate of error in

synthetic DNA sequencing is notably high, and the handing of DNA for research applications requires extreme care and environmental control.[27] In light of previous research, peptides are now considered a promising stabilizing ligand for nanoparticle synthesis due to their ease of production, specificity for inorganic materials, and tunability based on sidechain composition.

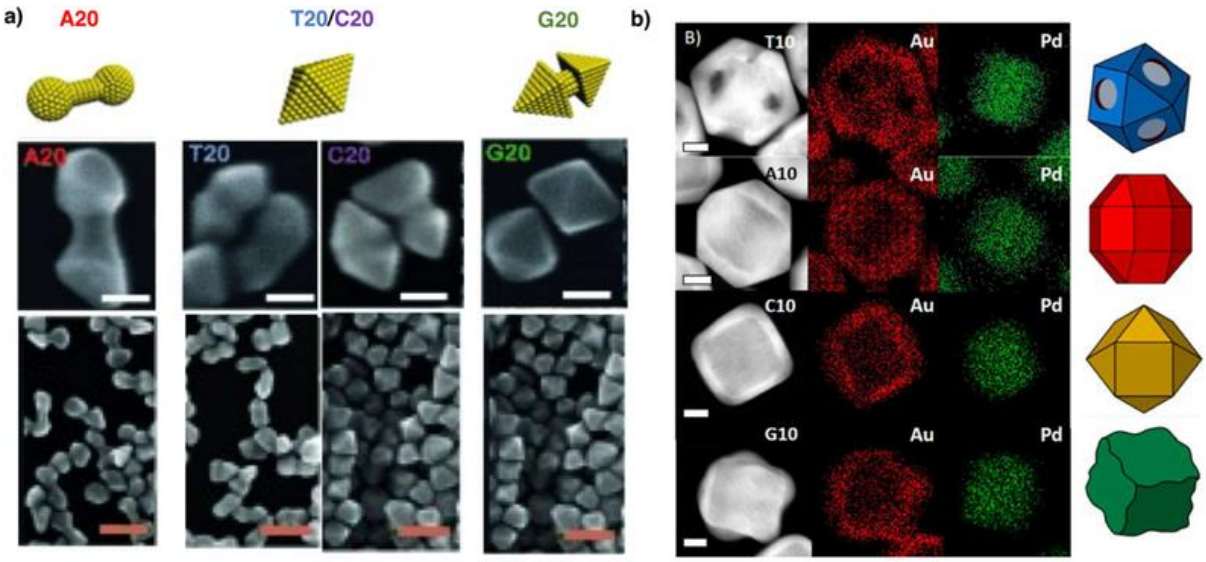

Figure 4. Inorganic morphologies of Au and Pd nanomaterials generated by DNA. (A) Base exchange at the 20th residue highlights the effect on the general Au nano structures. (B) Base exchange at the 10th residue produces fine alterations to the surface structures of Au and Pd nanoparticles. From reference 26.

1.5 Peptide ligands for nanoparticle synthesis

Peptides are non-toxic and environmentally friendly ligands with the capacity for biomolecular recognition.[6, 28] The peptide-based production of inorganic nanomaterials observed in nature offers inspiration for the rational design of synthetic ligands for industrial nanoparticle synthesis.[6] In 2012, researchers expanded upon this idea with their investigation of biomimetically prepared nanoparticles based on the peptide-mediated synthesis of nanomaterials by natural organisms.[6] Beyond their biochemical

specificity, peptides are also known to selectively interact with inorganic materials in order to construct intricate molecular structures, a process known as biomineralization.[29] For example, diatoms exist as unicellular micro algae organisms that extract silica from their environment in order to build intricate and diverse cell wall structures.[29] These nanoscale silicification processes incorporate specific low molecular weight silaffin peptides (silaffin-1A and silaffin-1B) which associate with and help induce precipitation of silica into nano-scale cellular structures (see Figure 5).[17] These peptides have inspired the design of a similar, synthetic R5 peptide (SSKKSGSYSGSKGSKRRIL) which is today widely used in peptide-driven silicification studies.[29] Additional biomineralization techniques have been investigated regarding magnetotactic bacteria which form magnetite crystals of consistent size and shape (see Figure 6).[18] In these peptide-mediated processes, nanoparticle growth is strictly controlled through interactions between the mineral and its specific peptides.[18] This suggests that synthetic materials-directed peptides may be inspired by those used in biomineralization processes and rationally designed to mimic this natural process.

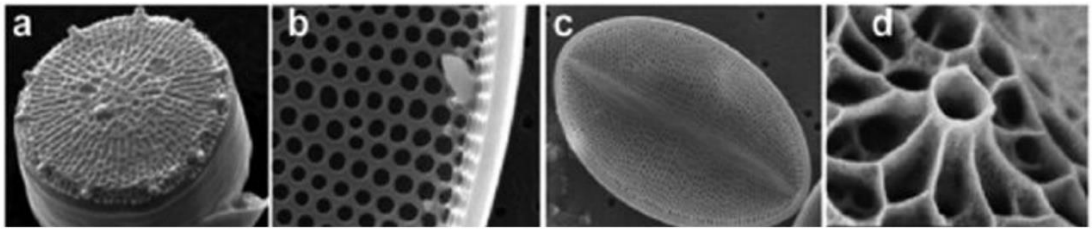

Figure 5. Silica-based nanostructures of diatoms found in nature. From reference 16.

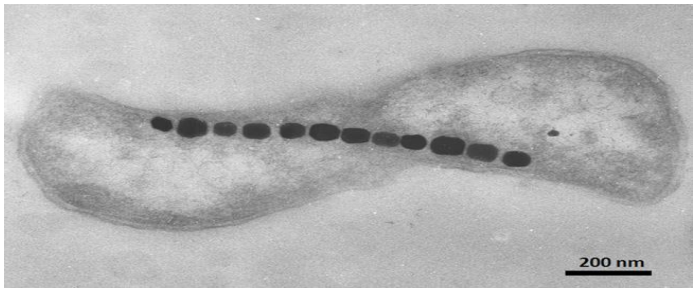

Figure 6. Magnetotactic bacteria containing magnetite crystals synthesized in a linear arrangement. From reference 17.

In recent decades, materials-directed peptides have proven to be extremely effective ligands for metal nanoparticles.[4, 6, 9] The biomimetic synthesis of palladium nanoparticles requires three key components: a solvent of synthesis, the Pd-specific Pd4 peptide, and a reducing agent. Figure 7 illustrates the typical sequence of events for nanoparticle synthesis, first highlighting the dispersion of Pd^{2+} atoms (blue spheres) and the Pd4 peptides (purple chains) in an aqueous solution. Research suggests that during this time it is likely that the peptides interact with the palladium to form a loose complex before reduction.[27] Next, sodium borohydride reduces Pd^{2+} to its highly active zero-valent state and initiates nucleation. The Pd4 peptides then recognize and coordinate to the face-centered cubic surface of growing Pd nanoparticles in solution.[9, 30] The nucleation process is arrested due to an increase in peptide-surface interactions which eventually cap and stabilize the nanoparticle in solution, preventing the accumulation of Pd atoms into Pd black which subsequently falls out of solution.[6] The unique sequence and structure of the Pd4 peptide determines its ability to consistently interact with the growing Pd NPs and successfully produce nanoparticles of consistent size and shape.

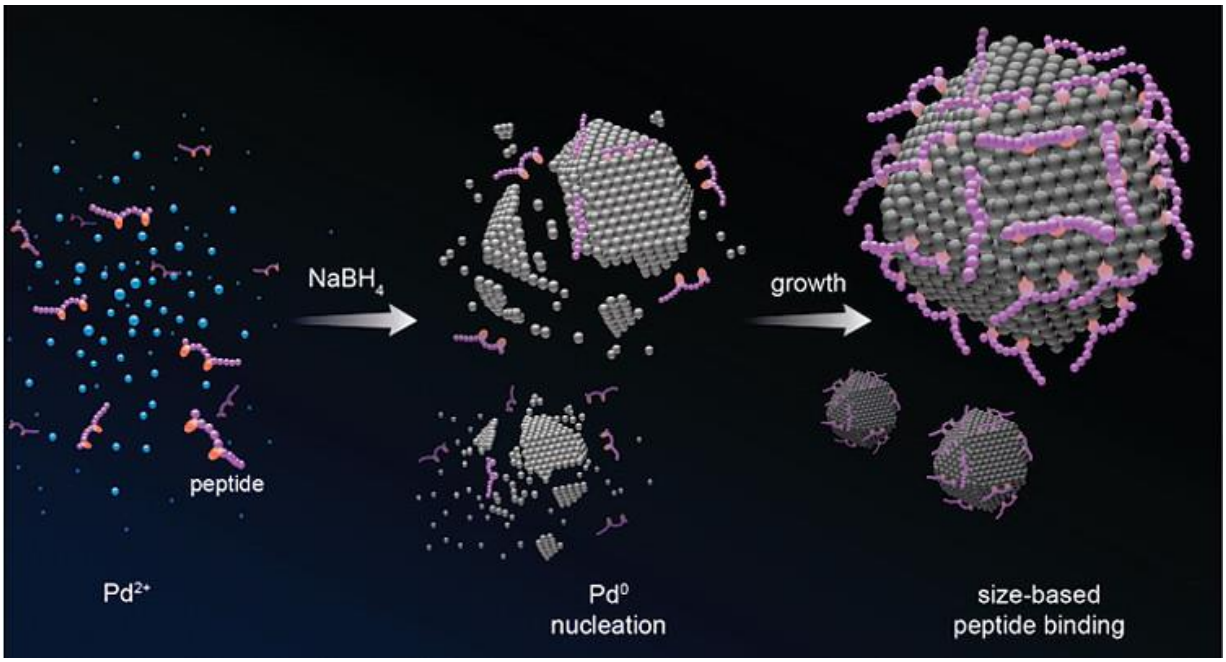

Figure 7. Schematic for peptide-mediated palladium nanoparticle synthesis in water. Left: Pd^{2+} atoms (turquoise) suspended in water with the Pd4 peptide (purple chain). Center: Reduction by sodium

borohydride initiates nucleation for the reduced Pd^0 atoms and the peptides begin to coordinate to the particle surface. Right: Continued particle growth and peptide binding on the surface results in a peptide-capped nanoparticle in solution. From reference 28.

1.5.1 Peptide specificity

Peptides that specifically bind to inorganic materials are often isolated through the application of biocombinatorial techniques such as phage display. The schematic in Figure 8 illustrates this process with a tin oxide example. [6,31] First, biopanning exposes the inorganic material to a library of peptides using a phage display technique in which a bacteriophage is manipulated to display various peptides of interest on its surface in order to expose it to the tin oxide nanosheet.[31] Washing steps serve to remove any peptides which have not displayed an interaction with the tin oxide nanosheet. The peptides that remain are then eluted, isolated, and amplified to highlight their specific affinity for the inorganic material of interest. This affinity often comes from specific residue interactions within the peptide, typically resulting in a particular orientation on the surface of the nanomaterial. Through the application of phage-display techniques, the Pd4 peptide, a hydrophilic dodecamer (TSNAVHPTLRHL), was isolated and shown to have unique specificity for palladium.[32] The location of amino acids within a peptide's sequence influences the overall binding activity and orientation of said peptide on an inorganic surface structure.[8, 30] Interactions with most transition metals depend on a ligand donor which has a free electron pair with which to occupy the d-orbitals. In recent decades, amino acids with the functional groups $-CO_2H$, -OH, -SH, $-NH_2$, and specifically ring nitrogens, have been shown to coordinate and direct growing nanoparticles into different morphologies.[27] Researchers have successfully determined which amino acids play a key role in the interaction between the Pd4 peptide and the Pd nanoparticle surface. Pandey et al. employed Monte Carlo modeling of the Pd4 peptide which verified binding activity at the two histidines in positions 6 and 11, creating a kinked structure on the palladium surface which serves to stabilize the growing nanoparticles in

solution (see Figure 9).[33, 34] This bidentate interaction and peptide orientation allows for exposed Pd on the nanoparticle surface which is crucial for catalytic activity.[33]

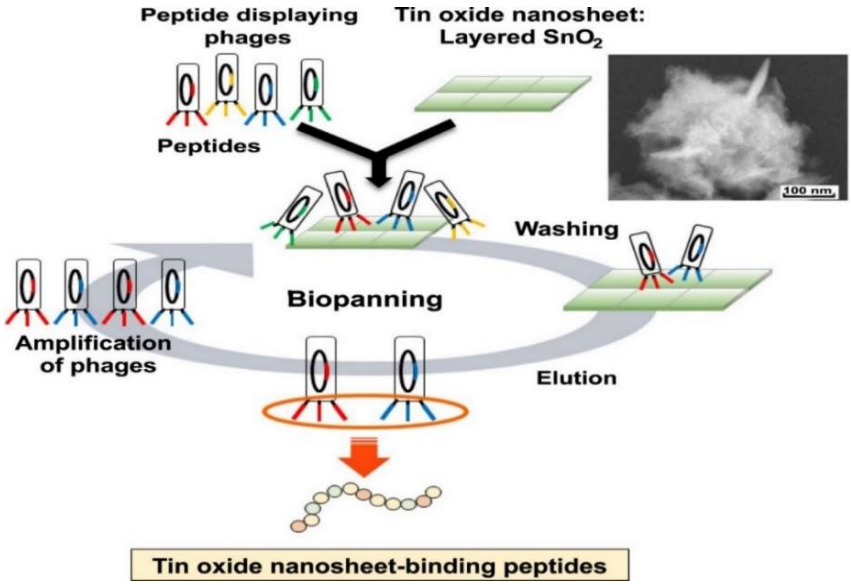

Figure 8. Schematic of phage display. Technique is here applied to a tin oxide nanosheet to isolate bound peptides showing specific affinity for tin. Washing employed a phosphate buffered saline and elution occurred in three steps: (1) high-salt buffer with 2M NaCl; (2) acidic buffer with 200mM Gly-HCl; and (3) high-phosphate-ion buffer with 500 mM NaH_2PO_4. From reference 31.

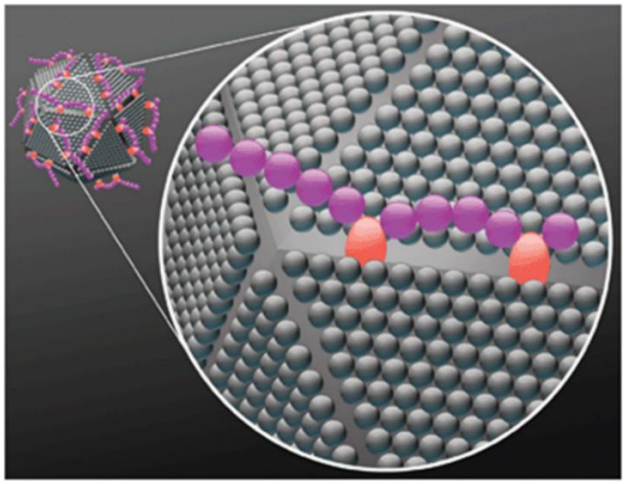

Figure 9. Depiction of the 'kinked' binding moiety of Pd4. Pd4 is shown as a purple chain with anchoring occurring via the histidines (red spheres) at positions 6 and 11. From reference 32.

1.5.2 Peptide tunability

Peptides are tunable and their specific residues, or side chains, may be manipulated to influence their function as a capping agent during the nucleation process of nanoparticle assembly.[6] This tunability allows researchers to ascertain the influence and significance of certain residues through amino acid substitution. As such, the amino acids critical to the peptides role in nanoparticle synthesis serve to inform the development of synthetic ligands designed with similar properties. Peptide sequences have been successfully altered to modify their binding activities, which influence the final size and shape of the nanostructures produced. For example, changing the 6, 11, or 6 and 11 histidines in the Pd4 peptide sequence to alanines results in nanoparticle size variations (see Table 1).[8]

Table 1. Peptide library with alanine substitutions at positions 6 and 11 with corresponding Pd NP sizes for various Pd/peptide ratios.

			Pd/peptide ratio size(nm)			
peptide	**sequence**	**pI[a]**	**1**	**2**	**3**	**4**
Pd4	TSNAVHPTLRHL	9.47	1.9 ± 0.3	1.9 ± 0.3	2.1 ± 0.4	2.0 ± 0.3
A6	TSNAV**A**PTLRHL	9.44	2.4 ± 0.6	2.1 ± 0.5	2.2 ± 0.7	2.1 ± 0.4
A11	TSNAVHPTLR**A**L	9.44	2.3 ± 0.4	2.4 ± 0.5	2.6 ± 0.4	2.4 ± 0.5
A6,11	TSNAV**A**PTLR**A**L	9.41	2.8 ± 0.7	3.0 ± 0.6	2.8 ± 0.7	3.1 ± 0.7

In addition to size, the shape and surface structure of nanomaterials can also be tuned in response to peptide sequence variations. Changes to the amino acid sequences of gold-binding peptides have been successfully leveraged to produce well-dispersed gold nanoparticles as well as gold helical superstructures.[35] The specificity of materials-directed peptides has also been employed to fine-tune the

crystal structures of growing nanoparticles. For example, Chiu *et al* employed two different platinum directed peptides on the same cubo-octahedral Pt 'seeds' to demonstrate their unique binding activity on specific facets or surfaces of the growing seeds.[36] The first peptide, T7 (TLTTLTN), selectively bound to Pt (100) facets, producing nanocubes. The second, S7 (SSFPQPN), bound to Pt (111) facets, producing nanotetrahedrons (see Figure 10). The number associated with the facets (100 or 111) highlight the amount of disorder on the faces of the crystals and correlate to the number of broken chemical bonds on that face (4 and 3 respectively).[36] Additionally, Rosi and colleagues found that the use of gold (Au) specific chiral peptides such as A3 may be tailored through sequence modifications and hydrophobic sequence additions to produce either helical nanoparticle assemblies or hollow spherical nanoparticles.[37-39] Finally, Matthew and colleagues generated atomistic modeling of gold nanostructures produced using the same A3 peptide as a stabilizing ligand in aqueous conditions.[40] The peptides' specific structure and binding strength at the biotic-abiotic interface during a period of particle growth indicate that the mechanism is limited by the stability of the anchoring peptides and their rates of adsorption.[40] There is thus a clear relationship between the specific amino acid sequence of materials binding peptides and the resulting shape and structure of the nanostructure it generates from inorganic material. This indicates that specific sequence changes may be engineered to materials-binding peptides to generate unique, fine-tuned nanostructures.

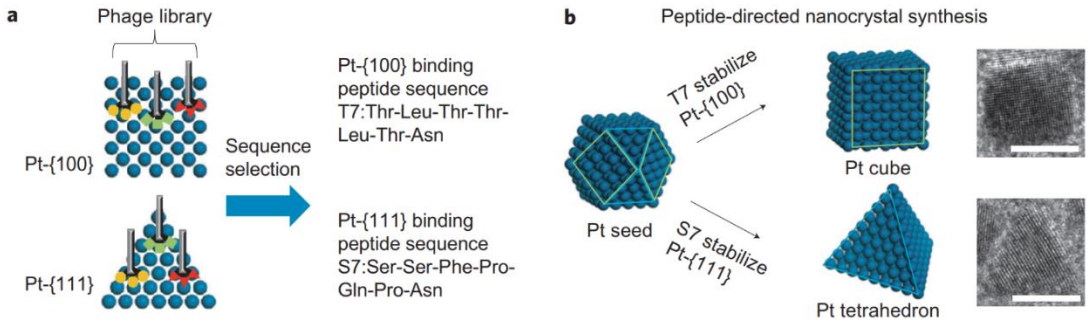

Figure 10. Schematic of the facet-directed peptide-mediated synthesis of platinum nanostructures. Synthesis applied materials-directed peptides T7 and S7 (b) which were isolated using phage display (a). From reference 36.

1.6 Peptide Capped Pd Nanoparticle Synthesis in Organic Solvents

The biomimetic synthesis of peptide-capped Pd NPs has revolutionized the nanocatalyst industry, boasting environmentally benign synthesis conditions and non-toxic ligand materials. However, all previous synthesis conditions for these nanoparticles have been aqueous. The Pd4 peptide is a hydrophilic dodecamer with multiple polar residues (see Figure 11). It dissolves easily in water and has thus been extensively studied in aqueous systems of biomimetic Pd NP synthesis. [8-10] However, in a world that depends heavily on petroleum, there remains a large number of reactions which require organic solvents, reagents, and specifically organic catalysts. This is where the aqueous synthesis of biomimetic peptide-capped Pd NPs falls short. Currently there is no research dedicated to translating biomimetic nanoparticle synthesis to organic systems. Innovations in this area would broaden the organic applications for these highly active, tunable, and environmentally benign nanocatalysts.

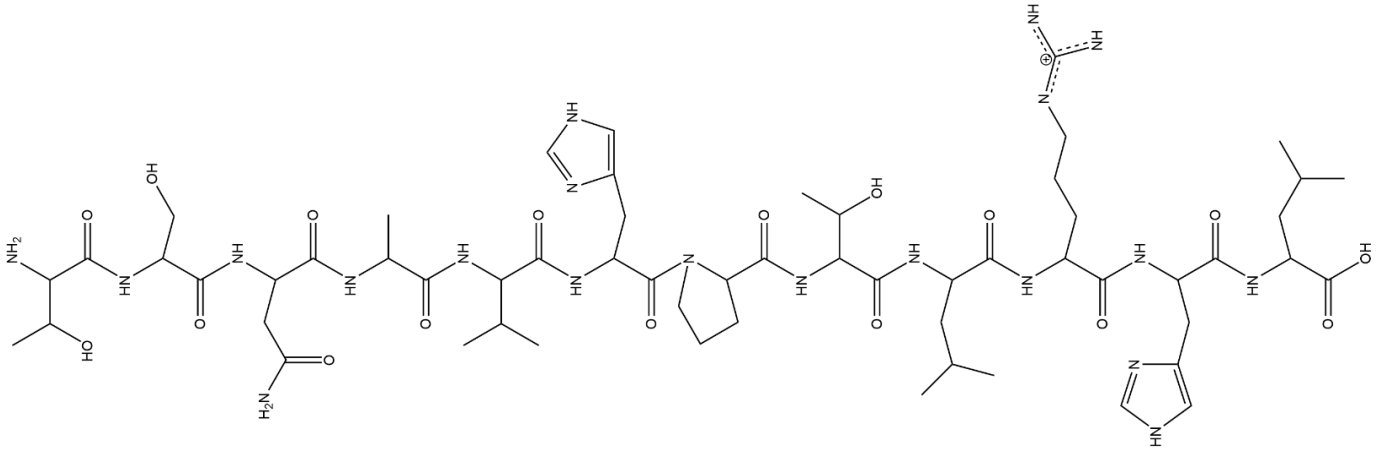

Figure 11. Chemdraw illustration of the Pd4 peptide (TSNAVHPTLRHL).

1.6.1 Bifunctional Peptides for Organic Applications

To better assess optimal green chemistry alternatives, various solvents are here investigated for biomimetic Pd NP synthesis. A solvent abundantly used in industrial Pd NP synthesis, dimethylformamide (DMF) is known for its ability to dissolve an array of compounds due to its polar aprotic nature.[5, 41] Highly

toxic, DMF poses serious threats to pollution of groundwater and soil composition as an industrial waste product and proper disposal incurs much scrutiny and high removal costs.[32] However, the highly polar and aprotic characteristics of DMF point towards possible less toxic alternatives. DMSO is a non-toxic polar aprotic solvent which may serve as a direct 'green' substitute to DMF in nanoparticle synthesis.[5, 42] In addition, ethanol is polar, protic, and capable of dissolving non-polar substances. It offers a baseline for non-toxic and versatile alternatives in organic nanoparticle synthesis. To translate the catalytic efficiency and minimal toxicity of Pd NP synthesis from aqueous to organic systems, the peptide used for synthesis must interact well with organic solvents. To this end, the Pd4 peptide is here combined with the S2 peptide, (AFILPTG) a heptamer with exceptional solubility in organic solvents which was deemed hydrophobic enough to operate well in both ethanol and DMSO (see Figure 12).[43] This peptide sequence was also determined as an ideal candidate for this system based on its affinity for silica. Previous work has also shown that peptides which display significant affinity for silica can also coordinate successfully with palladium as well.[44] As such, this peptide sequence is an ideal candidate for operation in organic solvents and likely does not negatively impact or negate the preferential palladium interaction by the Pd4 peptide upon its addition to it. These green systems are adapting the palladium-binding peptide Pd4 to incorporate this hydrophobic region on the -N terminus, -C terminus, and both N and C termini to aid in solvent interactions. These bifunctional peptides serve to translate the specificity and selectivity of biomimetic nanoparticle synthesis to organic systems which here employ either ethanol or DMSO as polar protic and polar aprotic solvents of synthesis, respectively.

Peptides likely cannot be sustainably upscaled for the industrial synthesis of Pd NPs. However, they lend insight to the structural characteristics needed to design synthetic ligands with similar affinity and selectivity for palladium. In order to apply the biomimetic synthesis of Pd nanoparticles to an industrial scale, synthetic molecules must be designed to mimic the functionality of the Pd-specific peptide to produce stable and active Pd NPs.

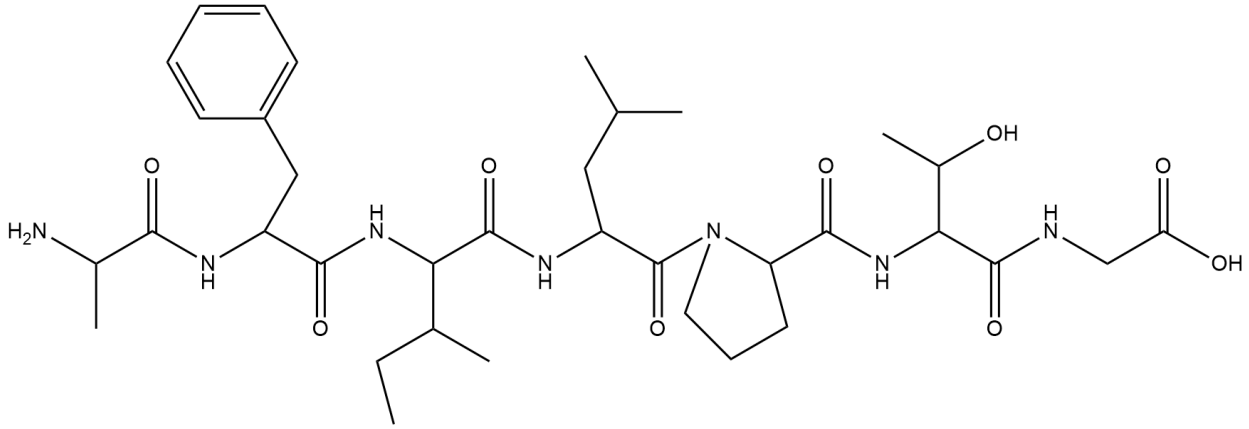

Figure 12. Chemdraw illustration of the S2 peptide (AFILPTG).

1.7 Pd Nanoparticles in Catalysts

Catalysis and fine chemical synthesis are extremely common and significant applications of Pd nanoparticles.[3] The formation of carbon-carbon bonds is an essential pathway for chemical transformations, especially when building value-added chemicals. The role of Pd nanoparticles in this realm of synthesis cannot be overstated. Pd NPs have proven extremely effective catalysts and have significantly lowered the necessary material loading for the most representative carbon cross-coupling reactions.[45] Among these, the Suzuki-Miyaura reaction is a technique considered essential to organic synthesis and the pharmaceutical industry overall (see Figure 13).[10, 46] Typically employing organometallic species that are non-toxic and affordable, the Suzuki transformation has reaction parameters which boast low energy input and operate under ambient conditions.[1] In the last decade, the Suzuki reaction was proven to be the second most utilized synthesis pathway for drug development, accelerating the coupling and functionalization process of pharmaceutical precursors such as biaryl moeities.[46]

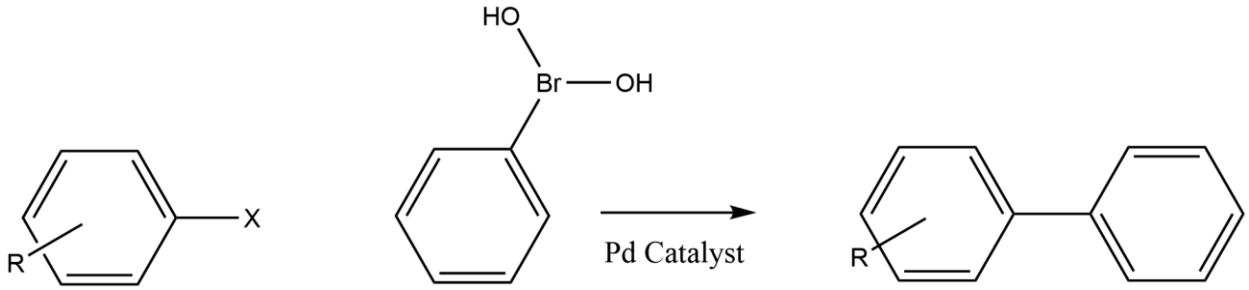

Figure 13. Basic line reaction for Suzuki-Miyaura carbon cross-coupling reaction. Far left species: R-substitued aryl halide (X). Center species: Phenyl-boronic acid. Far right species: Product of R-substituded bi-phenyl species with newly synthesized sp^2- sp^2 carbon bond.

1.7.1 Factors in catalytic activity

Catalyst activity of Pd NPs is influenced by a variety of factors, including size, shape, surface structure, agglomeration, and dispersity in solution. The peptide used in NP synthesis has a fine-tuned directing effect on growing metal nanoparticles (see 1.5.2), coating the surface and influencing both the atomic structure and the amount of exposed metal active sites. The size and structure of peptide-capped metal nanoparticles has been shown to directly influence their catalytic activity. This is a result of the unique crystal facets of the atomic configuration on the nanoparticle surface influencing its properties and activity as a catalyst.[16, 47] For example, in 2001 Xia *et. al* synthesized standard Pd nanocubes and concave Pd nanocubes using PVP as a stabilizing agent.[47] They demonstrated that the concave nanocubes had enhanced catalytic activity due to the high-index facets on the NP surface, verifying the significant influence that nanostructure variations have on overall reactivity. This concept was further investigated by Coppage and colleagues in their research on the influence of peptide sequence on NP size and reactivity.[8] The Pd4 peptide used for Pd NP synthesis was modified to substitute alanine for the histidine residues responsible for

anchoring on the Pd NP surface at positions 6 (A6), 11 (A11), and both 6 and 11 (A6,11).[8] These peptides in the order A6, A11, and A6,11, resulted in increasing NP diameters and decreasing catalytic activity as calculated through turnover frequency in the Stille C-C coupling reaction.[8] Coppage et. al further reinforced the practical tunability of peptide ligands in NP synthesis and their influence on the overall reactivity of generated nanoparticle catalysts.

1.7.2 Pd NP Catalytic Mechanism

The application of palladium in the Suzuki-Miyaura reaction has been extensively studied and the mechanism of action is well understood. While bulk Pd catalysts require an initial activation of Pd^{2+} to Pd^{0}, the Pd NPs stand ready to operate in their zero-oxidation state. The mechanism consists of three steps: oxidative addition (rate-limiting), transmetalation, and reductive elimination.[48] This reaction facilitates the comparison between the catalytic activities of the Pd NPs generated by different peptides in different solvents of synthesis.[10] The reaction may process in a homogeneous or heterogeneous manner when a nanoparticle is used (see Figure 14). Research using aqueous-based Pd4-capped nanoparticles in the Suzuki reaction have previously suggested the homogeneous mechanism occurs but testing using the ethanol and DMSO synthesized nanoparticles here were inconclusive.[10] Further testing would help to verify the specific mechanism for these systems.

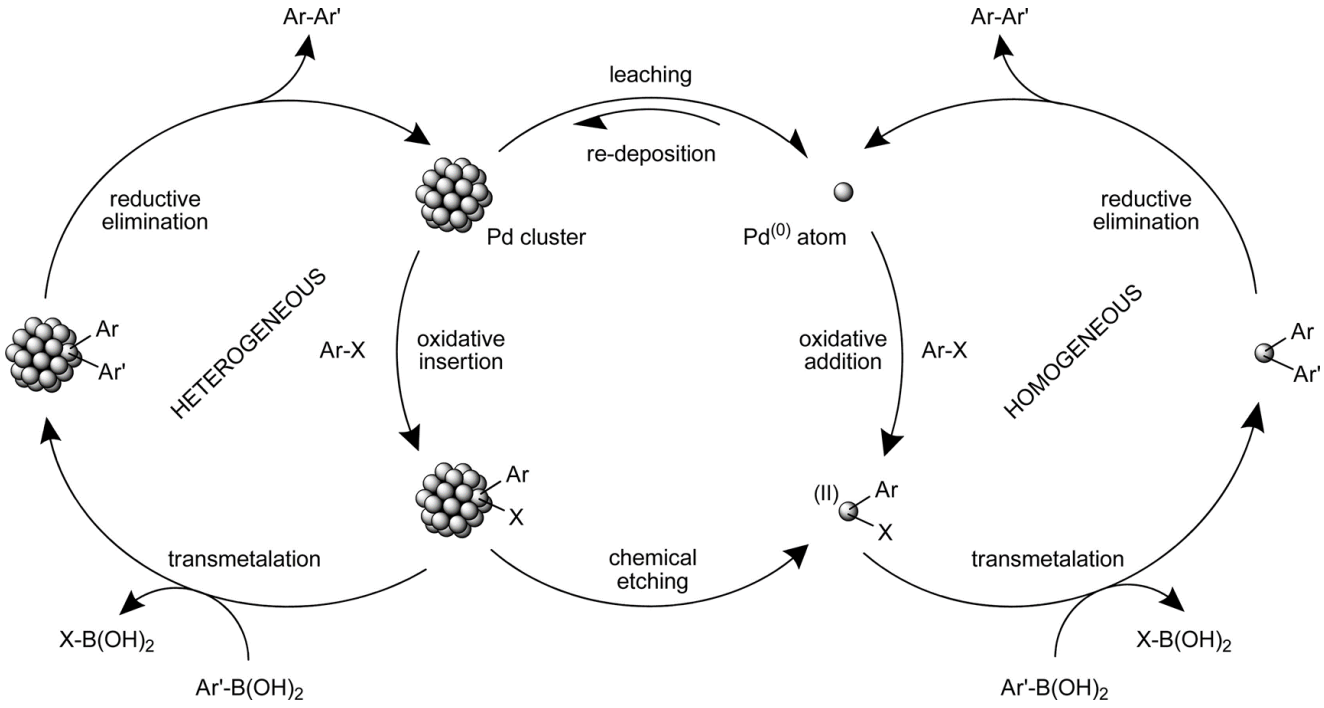

Figure 14. General schematic of the Suzuki-Miyaura mechanism for aryl-aryl coupling. The heterogeneous (left) and homogeneous (right) mechanisms are shown here. From reference 48.

CHAPTER 2

ETHANOL STUDIES

2.1 Method of Synthesis

The preparation of the Pd NPs occurred at room temperature on a benchtop and began by dissolving $Pd(OAc)_2$ in acetone to produce a 0.1 M solution of Pd^{2+} ions. This was added to a vial containing ethanol and a peptide solution (10 mg/mL in ethanol). Nanoparticles were synthesized using four different Pd:peptide ratios: 2:1, 4:1, 6:1 and 8:1. Two control peptides (S2 and Pd4) and three bifunctional peptides of interest (S2Pd4, S2Pd4S2, and Pd4S2) were investigated (see Table 2). All peptides were acquired from GenScript (Limerick, PA). Upon addition of the Pd^{2+} to the vial, complexation occurred between the peptide and the Pd^{2+} ions. After 25-30 minutes, the solution was analyzed via UV-Vis on an HP Agilent 8543 Spectrophotometer. Subsequently, a 0.1 M solution of the hydrazine, the reducing agent, in ethanol was added at 4 times molar excess to Pd^{2+}. Upon the addition of hydrazine, a color change from pale yellow to light brown was observed. The solution underwent reduction for one hour and was again analyzed via UV-Vis to verify the formation of nanoparticles. Post-reduction, the nanoparticles were left for 24 hours and visually inspected for any presence of precipitated Pd^0. Nanoparticles synthesized with all peptides in ethanol were observed for at least 24 hours for the precipitation of Pd black which indicates instability. All systems produced nanoparticles deemed stable enough to use for catalytic application.

Table 2. Amino acid sequences for two control and three bifunctional peptides used in NP synthesis.

Peptide	Amino Acid Sequence
Pd4S2	TSNAVHPTLRHLAFILPTG
S2Pd4	AFILPTGTSNAVHPTLRHL
S2Pd4S2	AFILPTGTSNAVHPTLRHLAFILPTG
S2	AFILPTG
Pd4	TSNAVHPTLRHL

2.2 Characterization of Nanoparticles in Ethanol

UV-Vis spectroscopy was used to characterize the nanoparticles post-complexation and post-reduction. The absorption spectra seen in Figure 15 indicates that there is an overall increase in absorbance for wavelengths greater than 300 nm. This is due to increased light scattering by the nanoparticles formed in solution. There is an observable trend across spectra in which decreasing concentration of peptide results in higher absorbance values. Data from the UV-Vis characterization suggests that stable nanoparticles were successfully formed in ethanol.

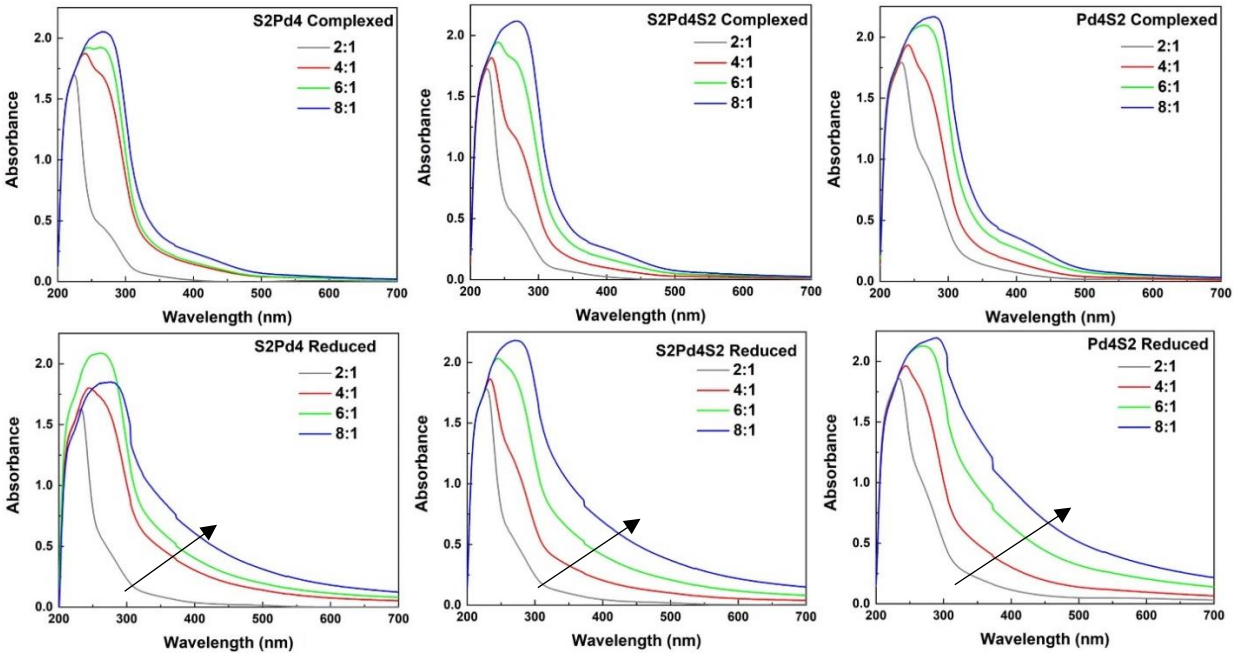

Figure 15. UV-Vis spectra (complexed and reduced) for Pd nanoparticles synthesized in ethanol. Nanoparticles were made with the bifunctional peptides S2Pd4, S2Pd4S2 and Pd4S2 and analyzed on a Shimadzu UV-2401 PC Spectrophotometer. Increased light scattering is highlighted with a black arrow.

Additional characterization was performed using transmission electron microscopy (TEM) in order to assess the size, shape, dispersion, and agglomeration of the nanoparticles. Images obtained for each major peptide and ratio are found in Figure 16. The Pd NPs indicate adequate dispersion and very minimal agglomeration. Nanoparticles were deemed to be spherical, and their average diameters were determined using the software, 'ImageJ' (sizing data is found in Table 3). In general, the average NP sizes increased as the concentration of peptide decreased.

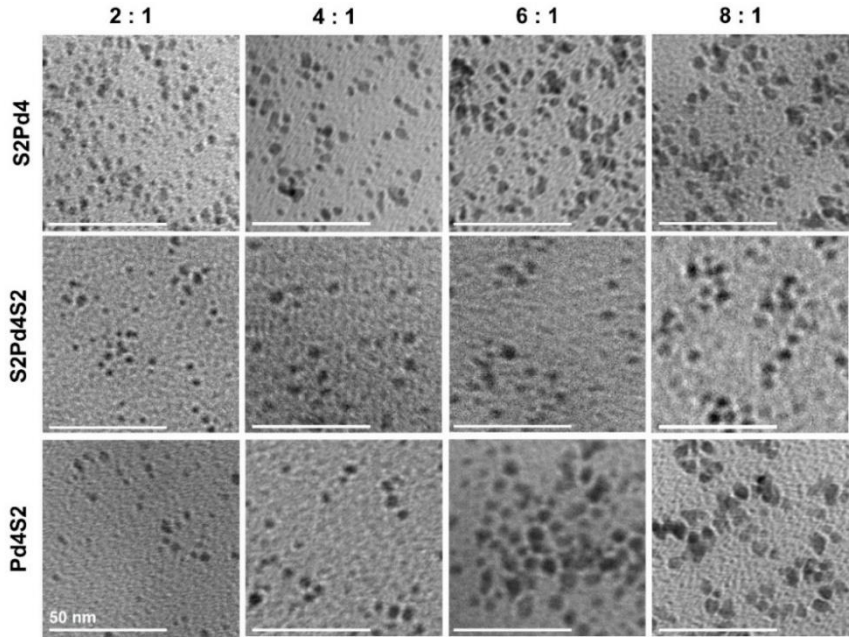

Figure 16. TEM images for Pd nanoparticles synthesized in ethanol. Nanoparticles shown here were synthesized from the three major peptides at their respective ratios and display a 50 nm scale bar. Particles are observed to be somewhat spherical and well dispersed, with slight agglomeration

Table 3. Average size determinations (nm) for Pd NPs synthesized in ethanol.

	2:1	**4:1**	**6:1**	**8:1**
S2Pd4	3.3 ± 0.9	2.9 ± 1.2	4.3 ± 1.3	4.6 ± 1.2
S2Pd4S2	3.6 ± 0.6	3.4 ± 0.7	3.7 ± 0.8	4.8 ± 0.7
Pd4S2	4.3 ± 1.9	3.6 ± 1.2	5.5 ± 1.7	5.8 ± 1.4
Pd4	2.9 ± 0.6	3.5 ± 0.7	2.8 ± 0.6	2.9 ± 0.9
S2	2.8 ± 0.7	2.9 ± 0.9	3.1 ± 1.1	3.2 ± 1.0

The formation of nanoparticles was successfully achieved in ethanol and characterized by UV-Vis, as observed by the general increase in absorbance seen at all larger wavelengths. In addition, TEM reveals rather spherical, monodisperse nanoparticles. It is also notable that the smallest size distribution is observed for the S2Pd4S2 peptide, which exhibited a high level of size control from the 2:1 to 6:1 ratios. This result is similar to previous aqueous studies done with the Pd4 peptide, which produced nearly equivalent particle sizes for ratios 2:1, 3:1 and 4:1.[30] In comparison, the NPs made using the S2Pd4 and Pd4S2 peptides displayed a trend in which the S2Pd4 peptide consistently produced smaller nanoparticles than the Pd4S2 peptide across all ratios. This is likely because in the Pd4S2 configuration the S2 peptide is positioned only two residues away from the histidine at position 11. Because this is one of two histidines responsible for anchoring the peptide, it is possible that the S2 peptide influences its ability to effectively coordinate to the palladium surface, thus consistently producing larger nanoparticles. Future modeling studies would clarify these observed trends and illustrate how each bifunctional peptide coordinates to the growing nanoparticle surface based on the position of the S2 peptide. When comparing the control peptides, the overall particle sizes are smaller than those prepared with the bifunctional peptides. The Pd4 peptide exhibits exceptional

size control for all ratios except 6:1 and the S2 peptide exhibits a consistent increase in particle size as peptide concentration decreases. The Pd4 peptide's strong affinity for Pd is maintained in ethanol and, although it produces very small nanoparticles (2.9 ± 0.6 nm), they are slightly larger than the ~ 2nm particles previously made in aqueous systems.[10, 30] Although the S2 peptide lacks histidine anchors, the amine groups on the peptide backbone orientate to Pd with minimal steric hindrance and interestingly produce the smallest nanoparticles overall (2.8 ± 0.7 nm).

2.3 Catalytic Application of Nanoparticles Synthesized in Ethanol

2.3.1 24-Hour Suzuki-Miyaura studies at 0.05 mol% Pd

The catalytic application of Pd NPs synthesized in ethanol was conducted using the Suzuki-Miyaura carbon cross coupling reaction. The reaction parameters mirrored previous studies conducted with Pd NPs synthesized in water (see Figure 17), so as to directly compare the catalytic effects derived from different peptides and solvents of synthesis.[10] First, 4-iodobenzoic acid and phenylboronic acid were dissolved in deionized water and K_3PO_4 (0.5 M, pH=6.7) in a 50 mL round bottom flask with an elliptical or egg-shaped stir bar. Subsequently, varying volumes of the peptide-capped Pd NPs in ethanol were added to the reaction to ensure a catalytic loading of 0.05 mol% Pd for all ratios with respect to the limiting reagent, 4-iodobenzoic acid. The flasks were covered with parafilm and left to stir for 24 hours undisturbed. The reactions were quenched with an aqueous solution of 5% hydrochloric acid. The product, 4-biphenyl carboxylic acid (BPCA), was extracted with ether and dried with a saturated NaCl solution followed by a treatment of anhydrous sodium sulfate. An internal standard (75 mg) was added to the solution before being dried on a rotovap. Quantitative analysis was achieved using a JEOL 300 MHz NMR. The internal standard, tert-butylphenol, (phenolic proton at $\delta = 6.75$ ppm) was manually integrated as a 100% yield. Subsequently, the product of 4-biphenyl carboxylic acid, (arene ring protons at $\delta = 8.17$ ppm) was integrated to assess the percent yield (see Figure 18). The verification of product formation was conducted via GC-MS in which

the product was silanated to replace the carboxylic acid proton with a trimethylsilane group to aid in separation (see Figures 19 and 20). The 24-hour studies were completed in triplicate for each peptide and ratio combination to determine average percent yields for major peptides (see Figure 21) and control peptides (see Figure 22). Although all three major peptides had similar yields, the S2Pd4S2 peptide resulted in the highest yield for all four ratios, with the greatest yield observed for the 4:1 ratio at 98.3 ± 1.2%. Overall, the bifunctional peptides had noticeably higher yields than the control peptides.

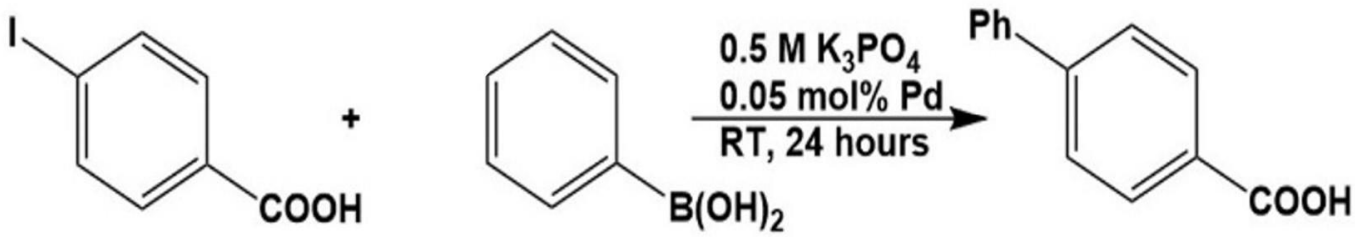

Figure 17. Specific parameters for the 24-Hr Suzuki-Miyaura reaction. Reaction was conducted in this work as described in section 2.2.1.

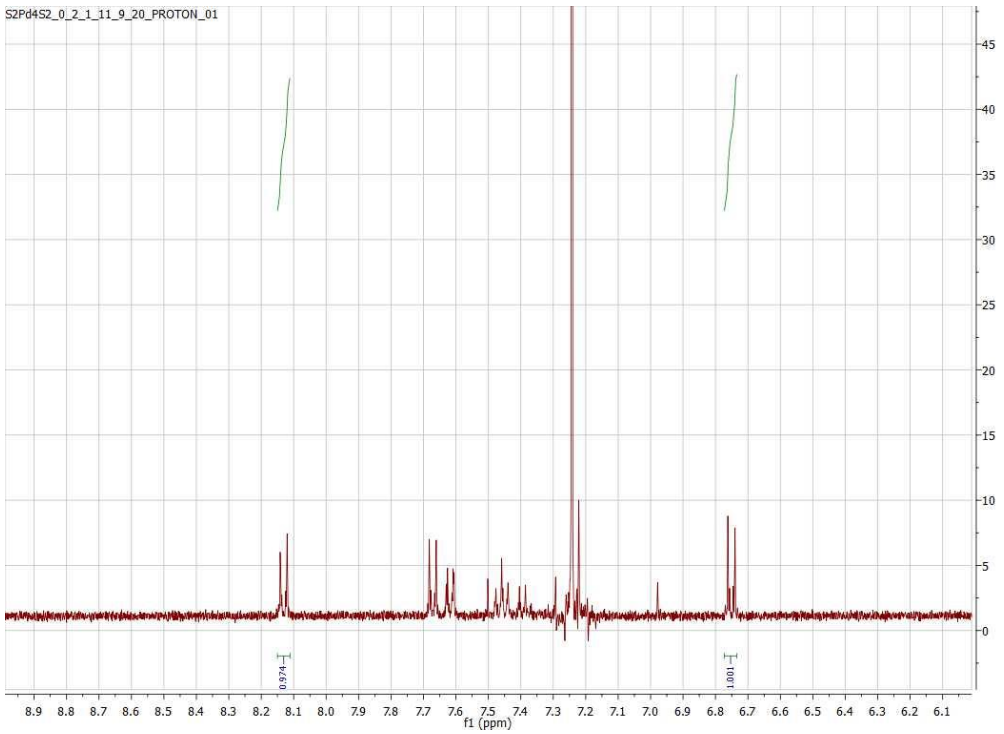

Figure 18. Single-pulse, proton NMR of 24-Hr Suzuki reaction utilizing Pd NPs synthesized in ethanol with the S2Pd4S2 peptide at a 2:1 Pd:peptide ratio. Image processed using MesReNova software.

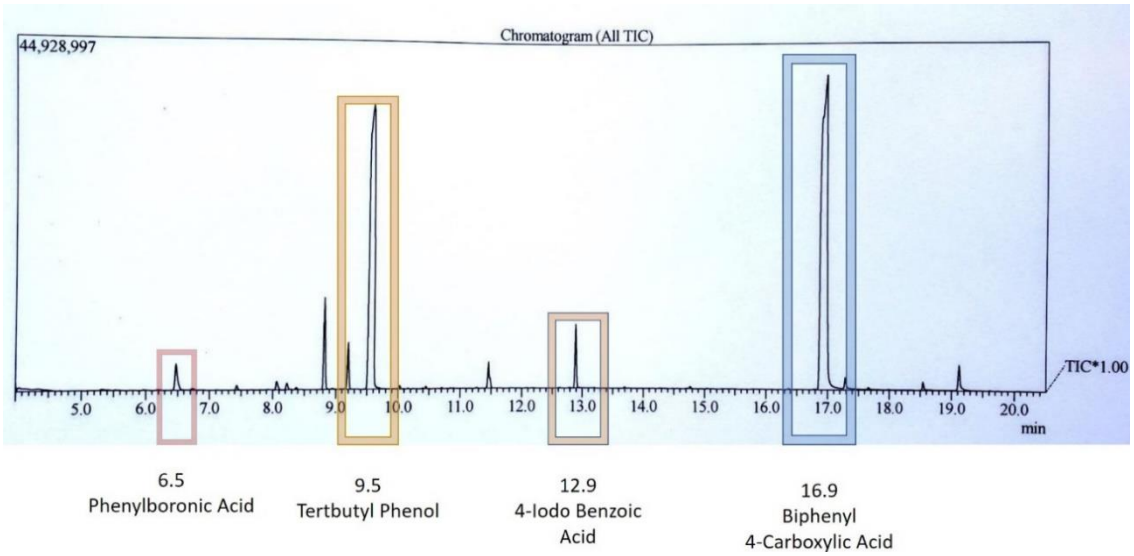

Figure 19. Verification of Suzuki product via gas chromatogram. Image generated from Shimadzu GC-MS QP2010 SE with relevant species identified.

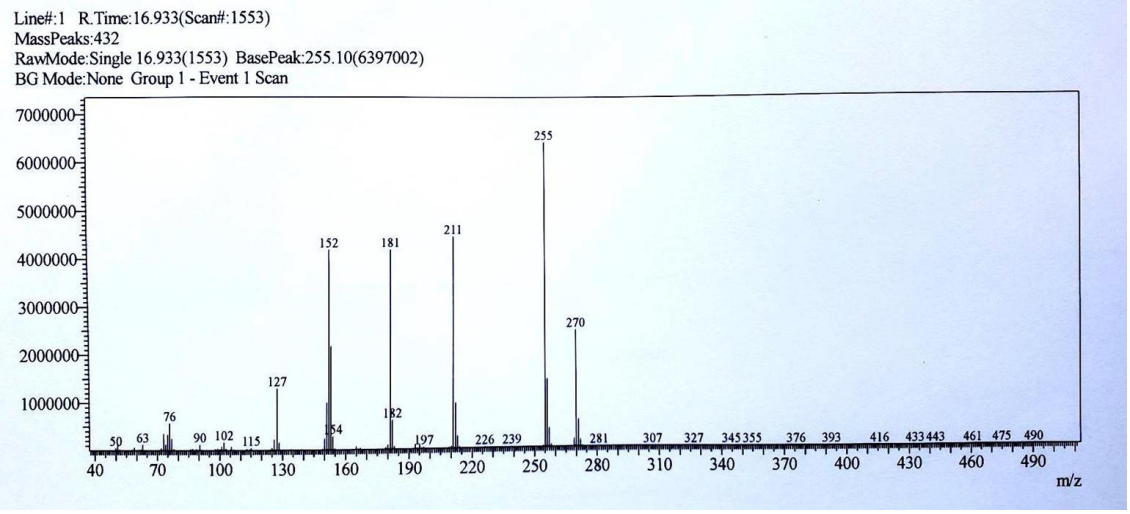

Figure 20. Verification of Suzuki product via mass spectrum. Image generated from Shimadzu GC-MS QP2010 SE. The image highlights the parent peak on the far right and the base peak immediately left of it. Masses correlate to the silylated product weight.

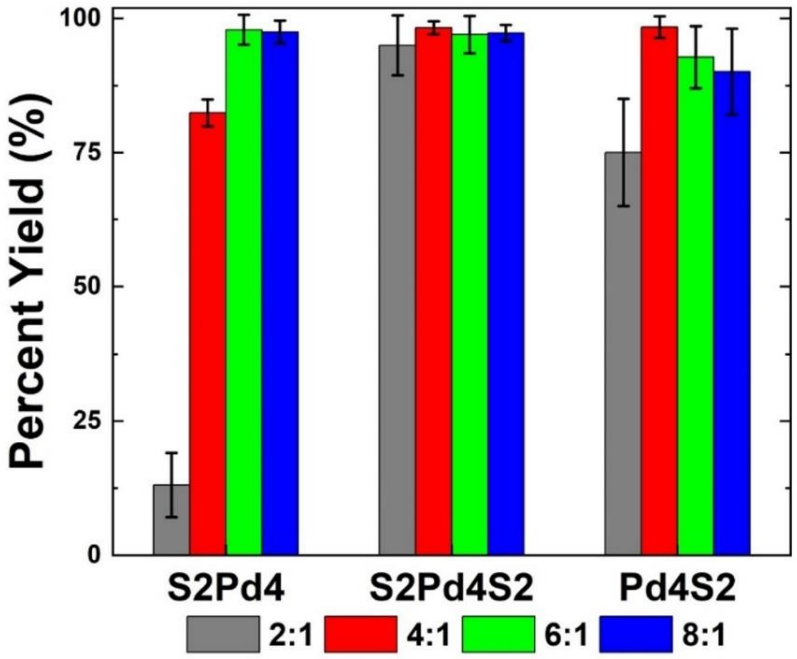

Figure 21. Average percent yields determined from the 24-hour Suzuki reaction using Pd NPs synthesized in ethanol from the three major peptides. Reactions were run in triplicate for each system.

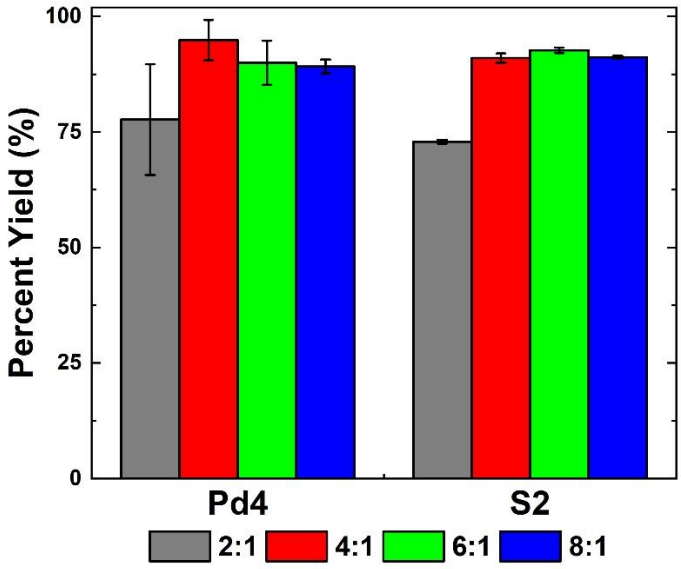

Figure 22. Average percent yields determined from the 24-hour Suzuki reaction using Pd NPs synthesized in ethanol from the two control peptides.

Peptide-capped Pd NPs synthesized in ethanol prove to be highly efficient catalysts in the Suzuki-Miyaura reaction. The results obtained for various peptide and ratio combinations indicate how the positioning of the S2 group and the concentration of peptide influence the overall yield. There was not a distinct trend of any one ratio resulting in overall greater yields than the others. The S2Pd4S2 peptide, however, produced the highest average percent yield across almost every ratio, indicating that it is an ideal bifunctional peptide for the translation of Pd NP synthesis to organic solvents. With two hydrophobic regions, the peptide likely interacts better with ethanol during NP synthesis than the peptides with only one S2 group, especially at the lower ratios. The 24-Hr Suzuki reaction was also conducted with unmodified control peptides. For S2 and Pd4 the average percent yield was lower than that of the S2Pd4S2 4:1 Pd NPs (98.3 ± 1.2), with the highest yields being 94.9% and 92.6% respectively. The affinity of Pd4 and its surface orientation allows for exposed Pd resulting in high percent yields. Interestingly, the S2 peptide, which has no specific Pd affinity, also exhibited significant yields. It is likely that the small particle size contributed to the high catalytic activity. Additionally, it is possible that the amine groups of the S2 peptide backbone

facilitated very weak, nonspecific binding on the NP surface, which may have diminished stability as a capping agent as compared to the stronger, more specific binding of the Pd4 peptide. Such a weak capping agent would likely allow for more Pd leaching or possibly Pd exposure on the NP surface during the reaction which translates to enhanced catalytic activity. The 24-hour data further confirms that the optimization of peptide-mediated synthesis in organic solvents is best served through the application of bifunctional peptides which are specific to both the solvent of synthesis and the inorganic material of interest.

2.3.2. Turnover Frequency (TOF) Studies of Suzuki-Miyaura Reaction (Ethanol)

The 24-hour studies gave insight into variations between the reactivities of Pd NPs synthesized with different peptide capping agents at different ratios. However, there is a general similarity in the percent yields for the major bifunctional peptides. The 24-hour studies do not paint a clear picture of the influence of the S2 group's positioning on the NPs' catalytic activity. To further elucidate the reaction kinetics for Pd NPs made in ethanol, the most reactive peptide and ratio combinations for the three major peptides (see Table 4) were determined from the 24-hour studies and analyzed in separate TOF studies. TOF studies were conducted by scaling up the 24-hour reaction 4-fold and taking aliquots over a 2.5-6-hour period in order to determine the rate of product formation over time ((mol BPCA / mol Pd) * hr^{-1}). Aliquots were quenched in the same manner as the 24-hr studies, extracted, given the same internal standard, and dried via rotovap. The subsequent NMR analysis provided percent yields for the aliquots over time which were plotted in excel (see Figure 23). Analyses in which the linear progression of the reaction was verified with an $R^2 \geq 0.9$ were used to determine the turnover frequency which is indicated by the value of the slope in the generated line equation. TOF studies were run in triplicate and the determined values are listed in Table 5. Additionally, the product yield at the 2.5-hour mark for each reaction system was compared in Table 6.

Table 4. Peptides and ratios synthesized in ethanol with the highest reactivity as determined by the 24-hour Suzuki studies.

Peptide	Pd: Peptide Ratio	Highest % Yield
S2Pd4	6:1	98.3 ± 2.6
S2Pd4S2	4:1	98.3 ± 1.2
Pd4S2	4:1	98.4 ± 2.0
Pd4	4:1	94.9 ± 4.4
S2	6:1	92.6 ± 0.6

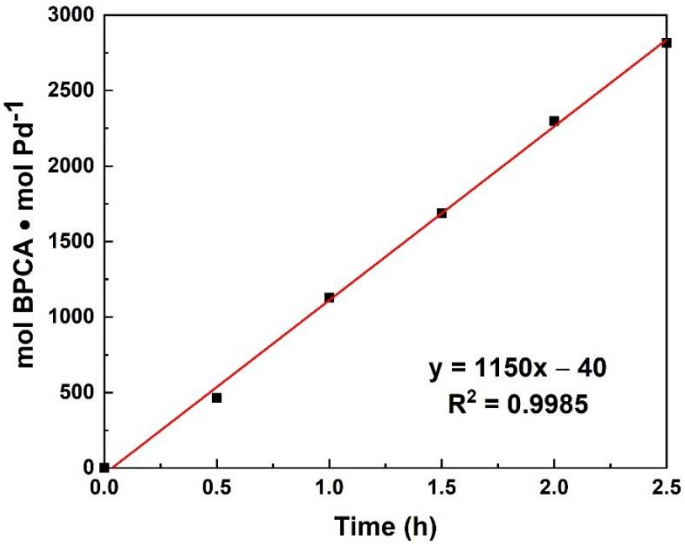

Figure 23. Graph of the linear progression of the Suzuki-Miyaura reaction over 2.5 hours. The Pd NPs were used at a loading of 0.05 mol% and synthesized in ethanol using the Pd4S2 peptide at a Pd:peptide ratio of 4:1. Percent yields for each aliquot were used to calculate the Y-values (mol BPCA / mol Pd) which were plotted against the X-values (Time in hours.).

Table 5. Turnover Frequency values for Pd NPs synthesized in ethanol. Optimal peptide ratios obtained from Table 4.

Peptide (Ratio)	TOF Value (mol BPCA / mol Pd) * Hr^{-1}
S2Pd4 (6:1)	1176 ± 241
S2Pd4S2 (4:1)	1271 ± 349
Pd4S2 (4:1)	1092 ± 55
Pd4 (4:1)	808 ± 68
S2 (6:1)	550 ± 11

Table 6. Average product yield at 2.5-hour mark for Pd NPs synthesized in ethanol. Optimal peptide ratios obtained from Table 4.

Peptide (Ratio)	% Yield of BPCA product
S2Pd4 (6:1)	42.6 ± 3.5
S2Pd4S2 (4:1)	45.3 ± 6.4
Pd4S2 (4:1)	33.7 ± 1.3
Pd4 (4:1)	25.6 ± 3.1
S2 (6:1)	41.7 ± 0.2

The calculated TOF values indicate that the S2Pd4S2 4:1 nanoparticles were the most reactive. This is consistent with the results from the 24-Hr studies, further verifying the exceptional adaptation of the S2Pd4S2 peptide to ethanol for NP synthesis. In addition, the S2Pd4 shows a slightly higher TOF value than the Pd4S2 peptide, suggesting that the influence of the S2 group on the nanoparticle size further affects the subsequent catalytic activity. The TOF values determined here are significantly higher than those

reported for a previous Suzuki study employing Pd4-capped NPs synthesized in aqueous conditions, (337 ± 93 mol product (mol Pd x h)$^{-1}$). Additionally, when comparing each peptide system at the 2.5-hour mark of the reaction, the TOF trends nearly mirror the observed product yields seen at that point in time. The higher reactivity for nanoparticles synthesized in ethanol may be due to favorable interactions between the added S2 groups and the ethanol solvent, increasing NP stability and catalytic efficiency. While the Pd4 peptide displays the lowest TOF as compared to the bifunctional peptides, it does demonstrate nearly twice the turnover frequency in ethanol than in water. Overall, the combination of hydrophobic resides on the peptide capping agent and an organic solvent of synthesis suggest favorable conditions for producing highly active and stable nanoparticle catalysts.

CHAPTER 3

DMSO STUDIES

3.1 Synthesis and Characterization of Nanoparticles in DMSO

The preparation of Pd NPs in DMSO followed the protocol outlined in 2.1 with only a variation in solvent. The peptide and hydrazine solutions were prepared in DMSO instead of ethanol, and the Suzuki reaction parameters remained the same as that which employed ethanol Pd NPs. Nanoparticles were characterized using the same techniques: UV-Vis was used to verify complexation and reduction (see Figure 24), and TEM allowed for NP visualization and sizing (see Figure 25). Only the average sizes of the most reactive DMSO Pd NPs were measured by hand and are listed in Table 7.

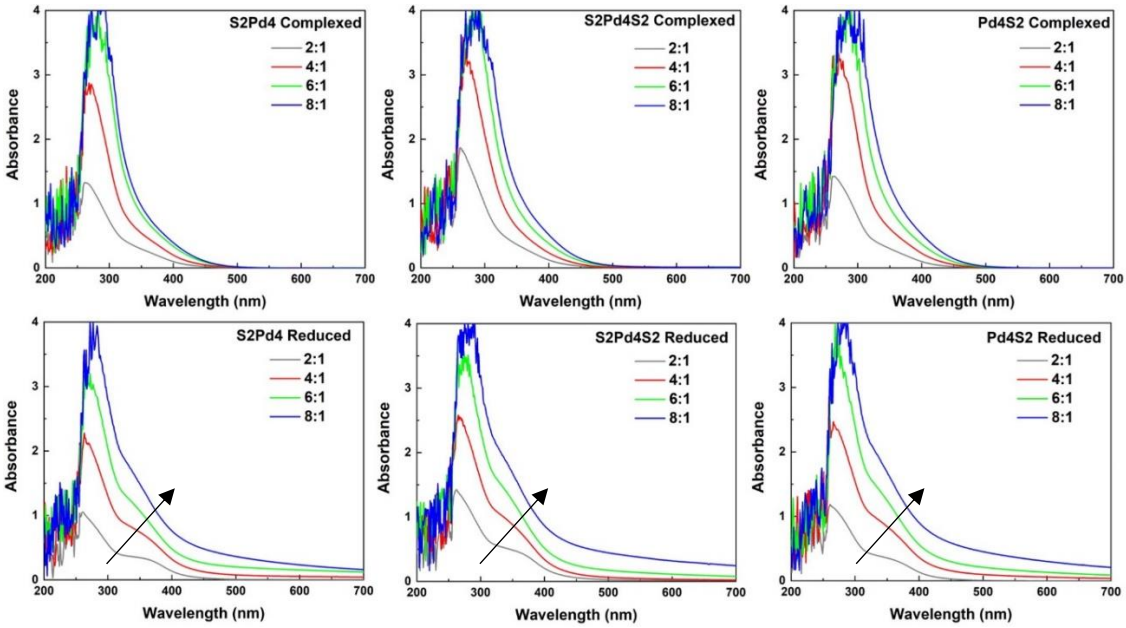

Figure 24. UV-Vis spectra (complexed and reduced) for Pd nanoparticles synthesized in DMSO. Increased light scattering is highlighted with a black arrow.

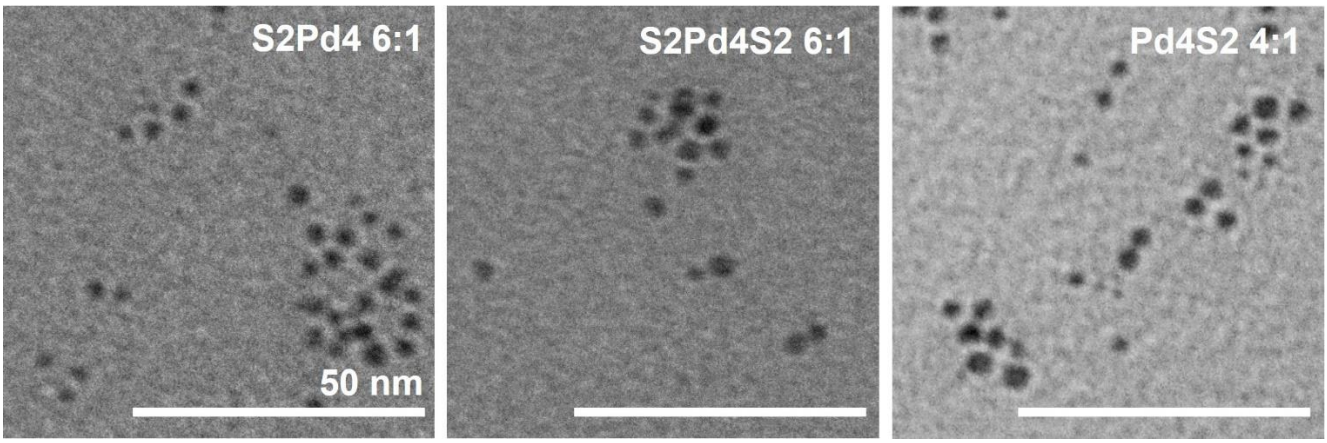

Figure 25. TEM images for Pd nanoparticles synthesized in DMSO. Synthesis was by the three major peptides and their respective optimal ratios with a 50 nm scale bar included in each image.

Table 7. Average size determinations (nm) for the most reactive Pd NPs synthesized in DMSO.

Peptide (ratio)	Average NP size (nm)
S2Pd4 (6:1)	3.2 ± 0.6
S2Pd4S2 (6:1)	3.0 ± 0.6
Pd4S2 (4:1)	4.3 ± 0.7

UV-Vis spectroscopy was successfully used to characterize the DMSO nanoparticles post-complexation and post-reduction. The absorption spectra seen in Figure 24 indicates larger absorbance values overall as compared to the spectra obtained for ethanol NPs. This may be due to the fact that the ethanol samples were run on a different UV-Vis instrument. The larger absorbance values seen in DMSO vs ethanol may also be due to additional interactions between the solvent and the Pd^{2+} in solution. There is also a very notable increase in absorbance for wavelengths greater than 300 nm which again suggests a

large amount of light scattering by the nanoparticles formed in solution. As seen in the ethanol NP spectra, there is a trend in which decreasing concentration of peptide results in higher absorbance values. Data from the UV-Vis characterization suggests that nanoparticles were successfully formed in DMSO.

The TEM analysis for the most active DMSO NPs first suggest a distinct difference in agglomeration as compared to the ethanol NPs. There is a notable amount of NP agglomeration which was not observed in the more equally dispersed ethanol TEM images. In addition, direct comparison of the same peptide and ratio combinations in ethanol suggests that the NPs made in DMSO are smaller for the S2Pd4 and S2Pd4S2 peptides and larger for the Pd4S2 peptide as compared to those made in ethanol. Among the three peptides, the S2Pd4S2 peptide produces the smallest NPs in DMSO. It is important to note that there are possible solvent interactions occurring between the DMSO and the palladium atoms on the NP surfaces during NP formation, affecting the final NP size. As seen in Figure 26, DMSO has in both of its resonance structures a lone pair of electrons on the center sulfur atom.[49] Because Pd^0 is a soft metal with vacant d-orbitals, sulfur, being 'soft' and having a lone pair of electrons, may potentially interact with the Pd atoms on the NP surface, occupying coordination sites that may otherwise be taken by the anchoring histidines on the Pd4 peptide. The Pd-DMSO interaction is considered labile and is thus constantly being 'formed' and 'broken'. During periods where coordination sites is vacated, bonds may be formed between the surface atoms or capping peptides of nearby nanoparticles, resulting in agglomeration effects.

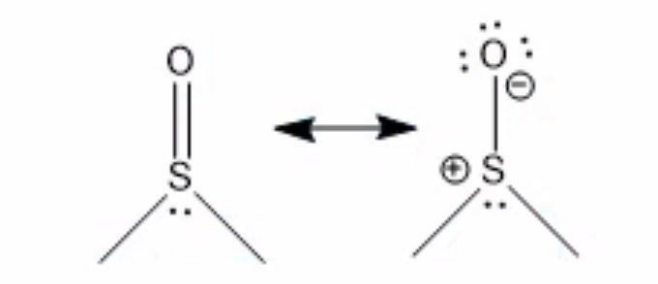

Figure 26. Resonance structures of DMSO.

3.2 Catalytic Application of Nanoparticles Synthesized in DMSO

3.2.1 24-Hour Suzuki-Miyaura Studies at 0.05 mol% Pd

The catalytic application of Pd NPs synthesized in DMSO followed the 24-hour protocol outlined in 2.2.1 with studies conducted in triplicate for each major peptide and ratio combination. NMR analysis was utilized to determine the percent yield after each 24-hour reaction (see Figure 27). Percent yields were determined for the major peptides (see Figure 28) and the control peptides (see Figure 29).

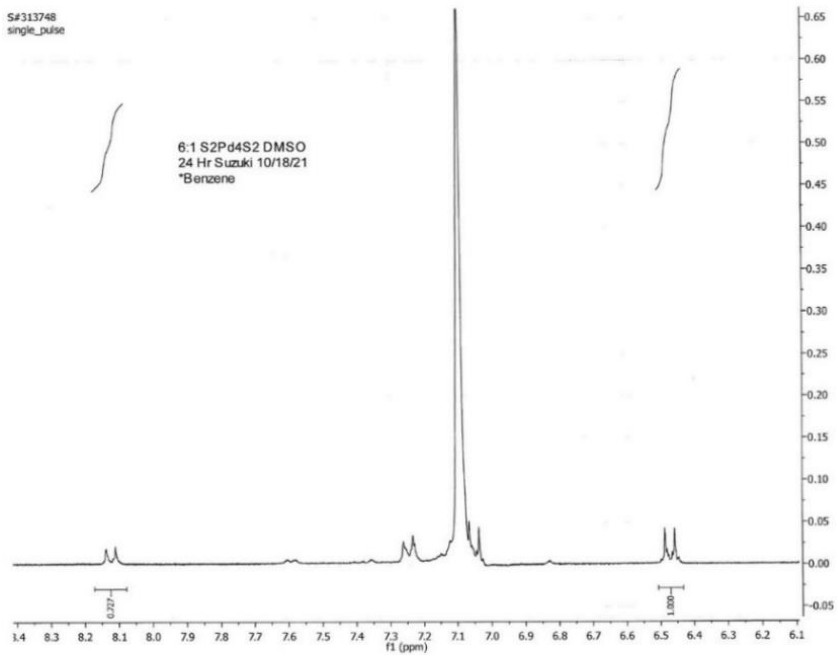

Figure 27. Single-pulse, high yield proton NMR of 24-Hr Suzuki reaction utilizing Pd NPs synthesized in DMSO. Synthesis was done with the S2Pd4S2 peptide at a 6:1 Pd:peptide ratio. Image processed using MesReNova software.

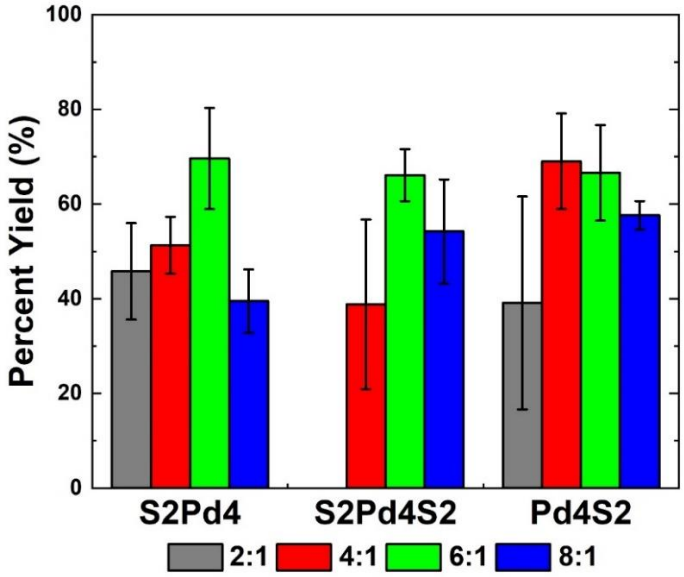

Figure 28. Average percent yields determined from the 24-hour Suzuki reaction using Pd NPs synthesized in DMSO from the three major peptides and their respective ratios.

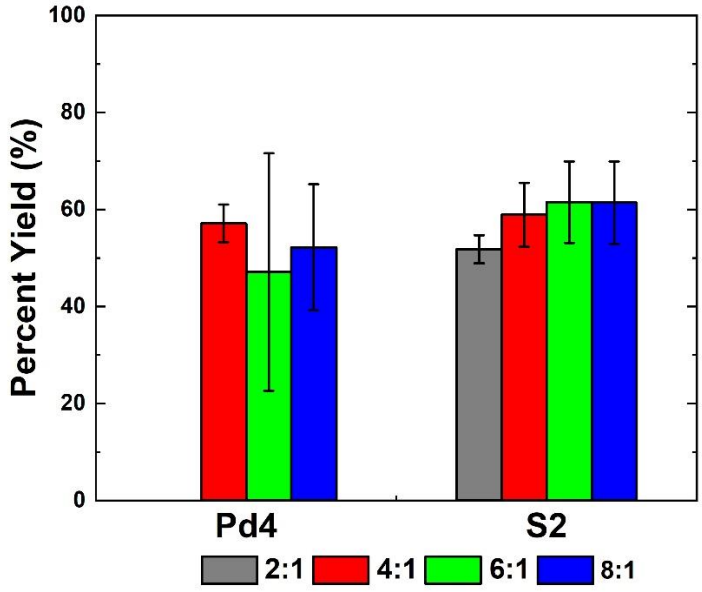

Figure 29. Average percent yields determined from the 24-hour Suzuki reaction using Pd NPs synthesized in DMSO from the two control peptides and their respective ratios.

When comparing the ratios of Pd:peptide, the 6:1 ratio produced consistently high yields with little differentiation between the major peptides. The S2Pd4, S2Pd4S2 and Pd4S2 reported very comparable yields, 69%, 66% and 69% respectively with error bars which overlap and indicate little distinction in yield. The general trend across peptides is that the product yield increases as the concentration of peptide decreases up to the 6:1 ratio for S2Pd4 and S2Pd4S2 and then declines with the 8:1 ratio. The Pd4S2 showed variation in this trend with the 4:1 ratio being the most active and the 6:1 ratio declining slightly from that. The control peptide S2 again displayed very high yields despite having no specific affinity for palladium. The Pd4 peptide did not show a distinct trend of activity based on peptide concentration. Generally, the 2:1 ratio reported the lowest yields across each peptide system. Interestingly, the 2:1 S2Pd4S2 and Pd4 NPs showed no activity, possibly due to the high concentration of peptide in solution. In this case it is possible that the surface of the NP becomes saturated with both peptides and the DMSO molecules, thus there would be very little Pd surface left exposed for reactivity.

When these results are compared to the 24-hour yields in ethanol, there is a significant overall decrease in catalytic activity as noted by the nearly 30% drop in product yield. This may be attributed to the fact that DMSO contains sulfur which is known to be a potential catalyst poison. Additionally, the DMSO molecules may occupy the orbitals of exposed Pd atoms on the NP surface and reduce the number of exposed active sites available for reactivity as compared to ethanol. Because there is not significant variability between the 24-hour yields among the bifunctional peptides, additional TOF studies are required to further illuminate the differences in catalytic activity as determined by the position of the S2 group on the peptide used for synthesis.

3.2.2. Turnover Frequency (TOF) Studies of Suzuki-Miyaura Reaction (DMSO)

The turnover frequency studies conducted in DMSO followed the same protocol outlined in 2.2.2 with studies conducted in triplicate for the most reactive peptide and ratio combinations. TOF values were determine for each combination (see Table 8) with an example TOF calculation shown in Figure 30. Additionally, the product yield at the 2-hour mark for each reaction system was compared in Table 9.

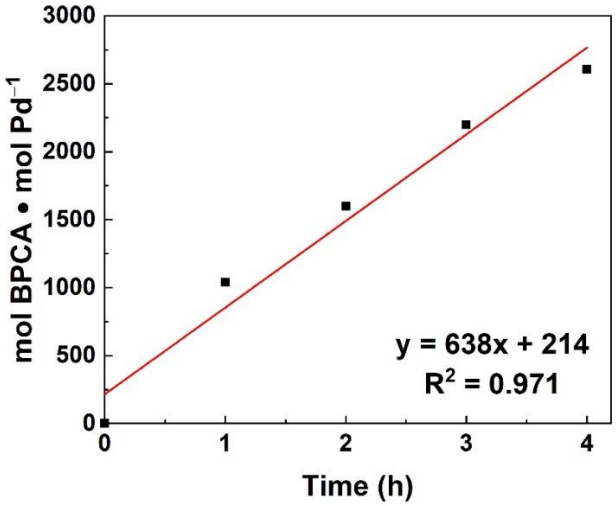

Figure 30. Graph of the linear progression of the Suzuki-Miyaura reaction over 4 hours. The Pd NPs were used at a loading of 0.05 mol% and synthesized in DMSO using the S2 peptide at a Pd:peptide ratio of 6:1. Percent yields for each aliquot were used to calculate the Y-values (mol BPCA / mol Pd) which were plotted against the X-values (Time in hours.).

Table 8. Turnover Frequency values for the Pd NPs synthesized in DMSO with optimal peptide and ratio combinations as determined by the 24-hour studies.

Peptide (Ratio)	TOF Value (mol BPCA / mol Pd) * Hr^{-1}
S2Pd4 (6:1)	262 ± 90
S2Pd4S2 (6:1)	394 ± 166
Pd4S2 (4:1)	260 ± 73
Pd4 (4:1)	289 ± 5
S2 (6:1)	599 ± 108

Table 9. Average product yield at 2-hour mark for Pd NPs synthesized in DMSO using optimal peptide and ratio combinations.

Peptide (Ratio)	% Yield of BPCA product
S2Pd4 (6:1)	9.1 ± 0.5
S2Pd4S2 (4:1)	9.9 ± 1.1
Pd4S2 (4:1)	8.6 ± 0.9
Pd4 (4:1)	8.2 ± 1.6
S2 (6:1)	21.5 ± 1.0

The calculated TOF values lend insight to the specific effects that capping agents have on the catalytic activities of the NPs produced. When comparing the bifunctional peptides, the S2Pd4S2 peptide again boasts the highest turnover frequency, followed by S2Pd4 and Pd4S2. This trend is consistent with the results of the ethanol TOF studies. Interestingly, the highest TOF value corresponds to the NPs produced

by the S2 peptide. The type of ligand interactions for the S2 peptide are likely limited to the amine groups on the peptide backbone and the DMSO molecules. When compared to the cyclic amine groups for the histidine residues on Pd4, these interactions are considered weaker because the cyclic amines can facilitate back-bonding from the Pd atoms whereas the amines on the peptide backbone cannot. As a result, the S2 ligand interactions are weaker in comparison to the peptides that feature Pd4 and may result in less stability on the NP surface and thus more potentially exposed active sites or leached Pd atoms available for reactivity. In addition, TEM images of the S2 nanoparticles in DMSO demonstrate a significant increase in the number of nanoparticles made with the 6:1 and 8:1 ratios as compared to the lower ratios (see Figure 31). This significant increase in nanoparticle concentration likely influences the high turnover frequency. It is likely that once the concentration of palladium exceeded the capping ability of the peptides in solution, the excess palladium in the system was capped by the available DMSO ligands which acted quickly and without any steric hindrance as compared to the S2 peptide. Thus, a significant number of Pd NPs with very weak or labile stabilizing agents characterize the S2 system at the 6:1 and 8:1 ratio and result in the highest TOF value. Generally, the TOF values calculated for the DMSO systems are significantly lower than those reported for the ethanol system. This is likely due to both the poisoning effect of sulfur in DMSO and the interactions of DMSO which occupy the NP active sites and diminish catalytic activity as compared to the ethanol system. Finally, when comparing each peptide system at the 2-hour mark of the reaction, the TOF trends nearly mirror the observed product yields seen at that point in time.

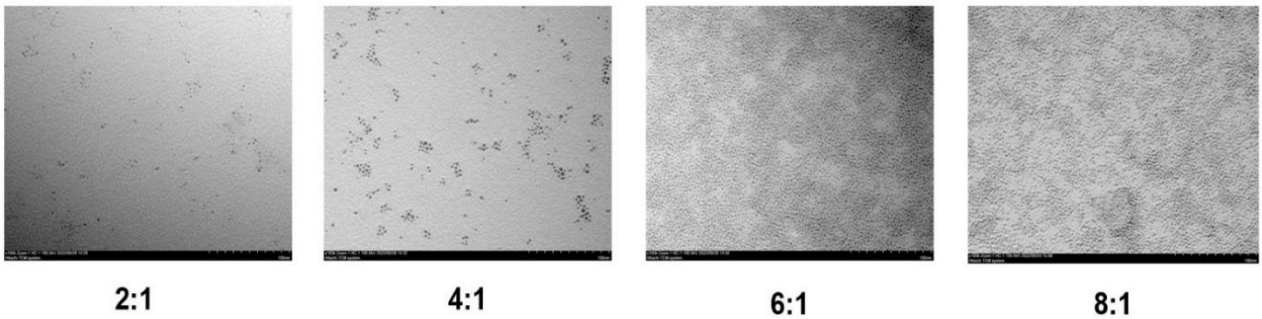

Figure 31. TEM images of nanoparticles produced by the S2 peptide in DMSO. Corresponding Pd : Peptide ratios are shown below. All images taken at a 100 nm scale.

CHAPTER 4

CONCLUSION

Natural ligand innovation in Pd nanoparticle synthesis is preferred for both environmental health and financial optimization. As such, the rational design of peptide-capped palladium nanoparticles is highly desirable and requires consideration of multiple factors such as stabilizing ligands and solvents of synthesis.[6, 8, 27, 30] Ligand innovation has verified that among natural and non-toxic ligands, peptides offer a specificity, tunability and practicality that significantly influences the efficiency of the catalytic nanoparticles produced.[5, 8, 24] First, peptide specificity creates NPs that are exceptionally efficient in catalysis. Nanoparticles produced with the Pd-specific Pd4 peptide significantly reduced the necessary catalytic loading in the Suzuki reaction from 1-5 mol% for NPs prepared with PVP and dendrimers to 0.05 mol%.[24-26] In addition, nanoparticle systems may be engineered to facilitate recyclability in the future, which significantly optimizes the usage of palladium in catalytic applications.[4, 50] Finally, peptides may be tuned to operate beyond the aqueous systems that current research is limited to. The peptides used here for nanoparticle synthesis were successfully designed to operate in organic systems by incorporating the functional group S2 to aid in solvent interaction without compromising the functionality and specificity of the Pd4 peptide.

Results from both the ethanol and DMSO studies suggest that the bifunctional peptides designed for operation in organic systems successfully synthesized stable Pd nanoparticles in their relative solvents of synthesis. Overall, TEM images indicate that the S2Pd4S2 peptide produces the second smallest nanoparticles in ethanol and the smallest nanoparticles in DMSO. However, the nanoparticles in ethanol were made at a 4:1 ratio for S2Pd4S2 while the smallest nanoparticles in DMSO were made at a 6:1 ratio for S2Pd4S2. It is possible that the interactions between DMSO and the Pd NP surface work in concert with a comparably lower peptide concentration to produce the smallest nanoparticles in DMSO. Further analysis

of additional TEM images for DMSO NPs will give a better understanding of how the peptide concentration and the peptide capping agent influence nanoparticle size, especially as compared to those prepared in ethanol. The 24-hour studies reveal that the most catalytically active nanoparticles are those prepared with either the 4:1 or 6:1 ratio of Pd:peptide in both ethanol and DMSO, suggesting that there are optimal peptide concentrations during synthesis which influence the catalytic activity of the Pd NPs they produce. Further, TOF studies revealed that among the bifunctional peptides, the S2Pd4S2 peptide-capped nanoparticles proved to have the highest turnover frequency. This is especially significant when the results are compared to previous aqueous systems. For example, previous work which applied Pd4-capped PdNPs synthesized in water at the same catalyst loading for the Suzuki reaction reported a TOF value of 337 ± 93 ((mol BPCA / mol Pd) * hr^{-1}). When compared to the Pd4-capped Pd NPs ethanol and DMSO, the values increase to 808 ± 68 and then decreases to 289 ± 5 ((mol BPCA / mol Pd) * hr^{-1}), respectively. In comparison, the S2Pd4S2-capped Pd NPs boasted noticeably higher TOF values in ethanol and DMSO, reporting 1271 ±349 and 394 ±196 ((mol BPCA / mol Pd) * hr^{-1}) respectively. Additionally, when comparing each peptide system at the 2-hour 2.5-hour mark of the reaction, the TOF trends nearly mirror the observed product yields seen at that point in time. Overall, the incorporation of the hydrophobic S2 group with the palladium specific Pd4 peptide on both the -N and -C termini results in nanoparticles with a 57.3% higher turnover frequency value in ethanol and a 26.6% higher turnover frequency value in DMSO when compared to the unmodified Pd4 peptide. This peptide is thus determined to be the most ideal candidate for transforming and optimizing the success of biomimetic peptide-mediated synthesis from aqueous to organic systems.

A final control study was also conducted which utilized Pd(OAc) as the catalyst species for the Suzuki reaction. The 24-hour product yields averaged 97.1 ± 0.86, which are very similar to the ethanol system. However, TOF studies indicated that the system reached roughly 60% yield within 30 minutes and a subsequent discoloration was observed for the remainder of the reaction. A black ring formed around the top of the round bottom flask and the solution turned dark grey. This suggests that the addition of palladium as a catalyst, when not in the form of a peptide-capped nanoparticle, results in the formation and

precipitation of palladium black. Additionally, there is a low probability of recovering free palladium when compared to the possibilities of designing nanoparticles for recoverability and recyclability as well.

Although additional data will contribute to a more complete understanding of peptide design, there are additional limitations that this current work should optimize in future directions as well. For example, the catalytic application of the Pd NPs in this work is the main method of comparison between NPs prepared with different bifunctional peptides. The aqueous Suzuki reaction system was here employed because it is a cornerstone system used previously for peptide-capped Pd NPs made in aqueous systems. Thus, there exists comparable records for the 24-hour reactions and TOF data obtained here. However, the Suzuki system is aqueous, and the nanoparticles applied in this work are suspended in organic solutions. It is possible that this research could be better optimized by applying the Pd NPs to a reaction system which employed the same solvent used in the nanoparticle synthesis, negating any unfavorable solvent interactions between the NPs and the reaction system. Additionally, the utilization of a polar aprotic solvent which does not have a soft, electronegative sulfur atom operating as a catalyst poison would be beneficial. Time constraints limited the sizing of the remaining TEM images for NPs prepared in DMSO which would have likely illuminated additional trends related to Pd:peptide ratios and the different bifunctional peptides. Finally, no modeling studies were applied to the NPs produced with bifunctional peptides or control peptides. This information would significantly increase understanding surrounding the influence of solvent on the peptides' functionality as they orientate to the nanoparticle surface.

Peptides are easy to design and are synthesized with precision. They are here successfully optimized for organic, biomimetic nanoparticle synthesis by simply altering their amino acid sequences. The various comparisons of Pd NPs made in this work illustrates how the rational design of peptide ligands influences the size, shape, and catalytic activity of the nanoparticles they produce. Although the upscaling of peptide-mediated synthesis is financially impractical, bifunctional peptides which have been optimized for organic systems will directly inform the design of synthetic ligands in the future, which will operate in affordable and scalable applications of organic biomimetic nanoparticle synthesis in an industrial setting.

REFERENCES

1. Biffis, A.; Centomo, P.; Del Zotto, A.; Zecca, M., Pd Metal Catalysts for Cross-Couplings and Related Reactions in the 21st Century: A Critical Review. *J. Am. Chem. Soc.* **2018,** *118* (4), 2249-2295.
2. Engle, K. M.; Yu, J.-Q., Developing ligands for palladium(II)-catalyzed C-H functionalization: intimate dialogue between ligand and substrate. *J. Org. Chem.* **2013,** *78* (18), 8927-8955.
3. Wang, B., A.; Godard, C.; Claver, C., Pdnanoparticles for C-C coupling reactions. *Chem. Soc. Rev.* **2011,** *10*, 4973-49895.
4. Cid, A., Simal-Gandara, J.; Synthesis, Characterization, and Potential Applications of Transition Metal Nanoparticles. *J. Inorg. Organomet. Polym.* **2019,** *30*, 1011-1032.
5. Biswas, T. Determination of Optimal Mild Organic Solvents of PdNPs for Carbon-Carbon Coupling Reactions. Georgia Southern University, University Honors Program Theses, 2019.
6. Briggs, B. D.; Knecht, M. R., Nanotechnology Meets Biology: Peptide-based Methods for the Fabrication of Functional Materials. *J. Phys. Chem.* **2012,** *3* (3), 405-418.
7. Benjamin, J., Palladium price forecast 2021: will the rally continue? 18 June 2021, 2021. https://capital.com/palladium-price-forecast-for-2021-and-beyond (Accessed July 2, 2022).
8. Coppage, R.; Slocik, J. M.; Briggs, B. D.; Frenkel, A. I.; Naik, R. R.; Knecht, M. R., Determining peptide sequence effects that control the size, structure, and function of nanoparticles. *ACS Nano.* **2012,** *6* (2), 1625-36.
9. Corra, S.; Shoshan, M. S.; Wennemers, H., Peptide mediated formation of noble metal nanoparticles—controlling size and spatial arrangement. *Curr. Opin. Chem. Biol.* **2017,** *40*, 138-144.
10. Briggs, B. D.; Pekarek, R. T.; Knecht, M. R., Examination of Transmetalation Pathways and Effects in Aqueous Suzuki Coupling Using Biomimetic Pd Nanocatalysts. *J. Phys. Chem.* **2014,** *118* (32), 18543-18553.
11. Table, P., Palladium. rsc.org. (Accessed July 2, 2022)
12. Palladium Mining. https://www.greatmining.com/palladium.html (Accessed August 23, 2022)
13. Garside, M. Global palladium consumption 2021. https://www.statista.com/statistics/693767/palladium-global-consumption-by-industry/. (Accessed June 18)
14. Egan-Morriss, C.; Kimber, R. L.; Powell, N. A.; Lloyd, J. R., Biotechnological synthesis of Pd-based nanoparticle catalysts. *Nanoscale Adv* **2022,** *4* (3), 654-679.
15. Britannica, T., palladium. In *Encyclopedia Britannica*, Britannica.com/science/palladium-chemical-element. (Accessed July 2, 2022)
16. Wang, F.; Li, C. H.; Sun, L. D.; Wu, H. S.; Ming, T. A.; Wang, J. F.; Yu, J. C.; Yan, C. H., Heteroepitaxial Growth of High-Index-Faceted Palladium Nanoshells and Their Catalytic Performance. *J. Am. Chem. Soc.* **2011,** *133* (4), 1106-1111.
17. Hildebrand, M., Diatoms, biomineralization processes, and genomics. *J. Chem. Rev.* **2008,** *108* (11), 4855-74.
18. Mirabello, G.; Lenders, J. J.; Sommerdijk, N. A., Bioinspired synthesis of magnetite nanoparticles. *Chem. Soc. Rev.* **2016,** *45* (18), 5085-106.
19. Saravanan, P., Gopalan, R., &Chandrasekaran,V.; Synthesis and Characterisation of Nanomaterials *Def. Sci. J.* **2008** 58 (4), 504-516.
20. Ostrom, A. C., Palladium-Based Nanomaterials: Synthesis and Electrochemical Applications. . *J. Am. Chem. Soc.* **2015,** 115(21), 11999-2044.
21. Martin, R.; Buchwald, S. L., Palladium-Catalyzed Suzuki−Miyaura Cross-Coupling Reactions Employing Dialkylbiaryl Phosphine Ligands. *J. Am. Chem. Soc.* **2008,** *41* (11), 1461-1473.
22. Aldrich, S., SAFETY DATA SHEET: Triphenylphosphine. sigmaaldrich.com, (Accessed July 17, 2022)

23. Sciuto, A. M.; Wong, B. J.; Martens, M. E.; Hoard-Fruchey, H.; Perkins, M. W., Phosphine toxicity: a story of disrupted mitochondrial metabolism. *Ann. N. Y. Acad. Sci.* **2016,** *1374* (1), 41-51.
24. Li, Y.; El-Sayed, M. A., The Effect of Stabilizers on the Catalytic Activity and Stability of Pd Colloidal Nanoparticles in the Suzuki Reactions in Aqueous Solution†. *J. Phys. Chem. B,* **2001,** *105* (37), 8938-8943.
25. Reetz, M. T. B., R.; and Wanniger, K., Suzuki and Heck reactions Catalyzed by Preformed Palladium Clusters and Palladium/Nickle Bimetallic Clusters. *Tetrahedron Lett.* **1996,** *37* (26), 4499-4502.
26. Kariduraganavar, M. Y.; Kittur, A. A.; Kamble, R. R., Chapter 1 - Polymer Synthesis and Processing. In *Natural and Synthetic Biomedical Polymers*, Kumbar, S. G.; Laurencin, C. T.; Deng, M., Eds. Elsevier: Oxford, 2014; pp 1-31.
27. Wang, Y.; Satyavolu, N. S. R.; Lu, Y., Sequence-Specific Control of Inorganic Nanomaterials Morphologies by Biomolecules. *Curr. Opin. Colloid Interface Sci.* **2018,** *38*, 158-169.
28. Briggs, B. D.; Li, Y.; Swihart, M. T.; Knecht, M. R., Reductant and Sequence Effects on the Morphology and Catalytic Activity of Peptide-Capped Au Nanoparticles. *ACS Appl. Mater. Interfaces.* **2015,** *7* (16), 8843-8851.
29. Senior, L.; Crump, M. P.; Williams, C.; Booth, P. J.; Mann, S.; Perriman, A. W.; Curnow, P., Structure and function of the silicifying peptide R5. *J. Mater. Chem. B* **2015,** *3* (13), 2607-2614.
30. Coppage, R.; Slocik, J. M.; Briggs, B. D.; Frenkel, A. I.; Heinz, H.; Naik, R. R.; Knecht, M. R., Crystallographic recognition controls peptide binding for bio-based nanomaterials. *J. Am. Chem. Soc.* **2011,** *133* (32), 12346-9.
31. Nakazawa, H. S., Y.; Hirose, T.; Masuda, Y, and Umetsu, M., Use of a Phage-Display Method to Identify Peptides that Bind to a Tin Oxide Nanosheets. *Protein Pept. Lett.* **2018** *25* (1), 68-75.
32. Pacardo, D. B.; Sethi, M.; Jones, S. E.; Naik, R. R.; Knecht, M. R., Biomimetic synthesis of Pd nanocatalysts for the Stille coupling reaction. *ACS Nano.* **2009,** *3* (5), 1288-96.
33. Pandey, R. B.; Heinz, H.; Feng, J.; Farmer, B. L.; Slocik, J. M.; Drummy, L. F.; Naik, R. R., Adsorption of peptides (A3, Flg, Pd2, Pd4) on gold and palladium surfaces by a coarse-grained Monte Carlo simulation. *J. Phys. Chem.* **2009,** *11* (12), 1989-2001.
34. Bhandari, R. C., R.; Kneckt, M.R., Mimicking nature's strategies for the desig of nanocatalysts. *Catal. Sci. Technol.* **2012,** *2*, 256-266.
35. Mokashi-Punekar, S.; Brooks, S. C.; Hogan, C. D.; Rosi, N. L., Leveraging Peptide Sequence Modification to Promote Assembly of Chiral Helical Gold Nanoparticle Superstructures. *Biochemistry* **2021,** *60* (13), 1044-1049.
36. Chiu, C.-Y.; Li, Y.; Ruan, L.; Ye, X.; Murray, C. B.; Huang, Y., Platinum nanocrystals selectively shaped using facet-specific peptide sequences. *Nat. Chem.* **2011,** *3* (5), 393-399.
37. Chen, C.-L.; Zhang, P.; Rosi, N. L., A New Peptide-Based Method for the Design and Synthesis of Nanoparticle Superstructures: Construction of Highly Ordered Gold Nanoparticle Double Helices. *J. Am. Chem. Soc.* **2008,** *130* (41), 13555-13557.
38. Chen, C.-L.; Rosi, N. L., Preparation of Unique 1-D Nanoparticle Superstructures and Tailoring their Structural Features. *J. Am. Chem. Soc.* **2010,** *132* (20), 6902-6903.
39. Song, C.; Zhao, G.; Zhang, P.; Rosi, N. L., Expeditious Synthesis and Assembly of Sub-100 nm Hollow Spherical Gold Nanoparticle Superstructures. *J. Am. Chem. Soc.***2010,** *132* (40), 14033-14035.
40. Yu, J. B., M. L.; Carri, G.A., A Molecular Dynamics Simulation of the Stability-Limited Growth Mechanism of Peptide-Mediated Gold-Nanoparticle Synthesis. *Univ. of Akrom* **2010,** *6*, 2242-2245.
41. Scientific, T. F., N, N-Dimethylformamide. In *SAFETY DATA SHEET*, Thermosfisher.com, 2018. https://www.thermofisher.com/search/browse/category/us/en/80014075/N%20N-Dimethylformamide?resultPage=1 (Accesed July 12, 2022)

42. Scientific, T. F., Dimethyl Sulfoxide. In *SAFETY DATA SHEET*, Thermofisher.com, 2019. https://www.thermofisher.com/order/catalog/product/A13280.36 (Accessed July 12, 2022)
43. Puddu, V.; Perry, C. C., Peptide adsorption on silica nanoparticles: evidence of hydrophobic interactions. *ACS Nano* **2012,** *6* (7), 6356-63.
44. Bedford, N. M.; Bhandari, R.; Slocik, J. M.; Seifert, S.; Naik, R. R.; Knecht, M. R., Peptide-Modified Dendrimers as Templates for the Production of Highly Reactive Catalytic Nanomaterials. *Chem. Mater.* **2014,** *26* (14), 4082-4091.
45. Cross-coupling reactions. In *Chemistry LibreTexts*, Lumenlearning.com, Vol. 25.5F. nptel.ac.in/courses/104101006/31 (Accessed July 26, 2022)
46. Buskes, M. J.; Blanco, M.-J., Impact of Cross-Coupling Reactions in Drug Discovery and Development. *Molecules* **2020,** *25* (15), 3493.
47. Zhang, Y.; Lyu, Z.; Chen, Z.; Zhu, S.; Shi, Y.; Chen, R.; Xie, M.; Yao, Y.; Chi, M.; Shao, M.; Xia, Y., Maximizing the Catalytic Performance of Pd@Aux Pd1-x Nanocubes in H2 O2 Production by Reducing Shell Thickness to Increase Compositional Stability. *Angew Chem Int Ed Engl* **2021,** *60* (36), 19643-19647.
48. Miyaura, N.; Suzuki, A., Palladium-Catalyzed Cross-Coupling Reactions of Organoboron Compounds. *Chem. Rev.* **1995,** *95* (7), 2457-2483.
49. Reynolds, W. R., Dimethyl Sulfoxide in Inorganic Chemistry. *Prog. Inorg. Chem.* **2007,** *12* (1), 1-99.
50. A. V. Dubey, A. V. K., A Bio-Inspired Magnetically Recoverable Palladium Nanocatalyst for the Ullmann Coupling reactiong of Aryl halides and Arylboronic acids In Aqueous Media. *Appl. Organomet. Chem.* **2020,** *34*, e5570-e5571.